University of Tartu

Faculty of Science and Technology

Institute of Physics

Physics department

Siim Heinsalu

Raman scattering from organic molecules deposited on the noble metal nanoparticles and graphene

Master degree thesis (30 EAP)

Supervisor: PhD Leonid Dolgov

Tartu 2017

TARTU ÜLIKOOL

Raman scattering from organic molecules deposited on the noble metal nanoparticles and graphene

Master's thesis
Siim Heinsalu

Abstract:

The rapid development of nanotechnologies, especially methods of synthesis of metal nanoparticles, preparation of nanostructured surfaces and atomically thin two-dimensional materials such as graphene renewed the interest to the Surface Enhanced Raman Scattering (SERS). The effect of Raman scattering was discovered a long time ago and has been associated with the part of scattered light, which changes the frequency after the interaction with molecular vibrations. The part of such non-elastically scattered light is usually small, because of the low cross section for the Raman scattering. Nanosized features on the substrate, on which this organic molecule is deposited, can work as an optical plasmonic antenna for the incident and scattered light and by such a way increasing the efficiency of the Raman process in several orders. Another mechanism, which can influence the polarizability of molecules on nanosurface, and, as consequence, Raman signal, can be connected with the resonant transfer of electrons from the substrate to the analyzed molecule. Questions connected to a molecular selectivity of SERS and the separation of its electromagnetic and charge transfer contributions are still under investigation nowadays.

Examples of both plasmonic and electron transfer influence on the Raman signals from the organic molecules deposited on graphene and nanosized noble metal nanoparticles were investigated in this work. Particularly graphene enhanced Raman scattering was detected for the adenine layer and compared with the SERS signal from adenine deposited on the surface previously decorated by noble metal nanoparticles. Surface enhanced Raman detection and assignment of spectral bands for adenine as a DNA constituent could be potentially important for those biomedical applications, in which monitoring of molecular conformations in DNA and its constituents would be essential.

Keywords: SERS, GERS, Raman Spectroscopy, noble metal nanoparticles, adenine

Raman hajumine orgaanilistelt molekulidelt sadestatud väärismetall nanoosakestele ja grafeenile

Magistritöö

Siim Heinsalu

Abstrakt:

Kiire nanotehnoloogia areng, eriti metallist nanoosakeste sünteesimise meetodite vallas ning nanostruktuursete pindade ja atomaarselt õhukeste kahedimensionaalsete materjalide sünteesimises nagu grafeen ja MoS_2 on suurendanud huvi pindergastatud Raman hajumise vastu (SERS). Raman hajumise mõju avastati kaua aega tagasi ja seda seostati hajunud valgusega, mis muudab oma sagedust molekuli vibratsioonide interaktsioonide tõttu. See mitte-elastne hajunud valguse osa on tavaliselt väike, kuna molekulide ristlõiked on Raman hajumise korral väikesed. Substraat, millele antud orgaaniline molekul on sadestatud, saab toimida kui optiline plasmooniline antenn ergastatud ja hajunud valgusele, millega Raman hajumine on tõhustatud mitme astme võrra. Teine mehhanism, mis saab mõjutada molekulide polaarsust nanopindadel, mis omakorda mõjutab Raman hajumist, on seotud resonantse elektronide ülekandega uuritud molekuli puhul. SERS-i jaoks molekulide valimine ning nende elektromagnetilised ja laengu ülekandega seotud mõjud on veel uurimise all.

Antud töös on uuritud näiteid nii plasmoonilise kui ka elektroonse ülekande mõjudest Raman hajumisele orgaanilistelt molekulidelt sadestatud grafeenil ja väärismetall nanoosakeste puhul. Eriline rõhk on grafeenergastatud Raman hajumise mõõtmisel adeniini kihilt ja selle võrdlemine SERS signaaliga adeniinilt deponeeritud pinnale, kuhu on eelnevalt paigutatud väärismetallnanoosakesed. Pindergastatud Raman hajumise mõõtmisel ja spektri piikide määramisel adeniinile DNA koostisosana võib olla potentsiaalne tähtsus biometitsiini aplikatsioonidele, kus DNA ja tema koostisosade jälgimine on eriti tähtis.

Märksõnad: SERS, GERS, Raman spektroskoopia, väärismetall nanoosakesed, adeniin

Table of contents

1. Introduction to Raman spectroscopy and methods to improve Raman signal intensity.

1.1 Raman spectroscopy: basics

When discussing the topic of light scattering, elastic light scattering is usually meant: the light interacts with the material during a very short time ~10^{-14} s and it becomes reflected or scattered without any changes in energy (frequency). It is also possible that one photon from 10 millions of other photons could be scattered inelastically with some very small decrease or increase in energy (frequency). The change in energy is caused by the interaction of light with valence bonds of atoms in the molecules. The continuous thermal motion of atoms in the molecule can be represented as their vibrations or rotations near the equilibrium positions (Fig.1). These vibrations, which can be described together with the specific symmetry of investigated crystal lattices or separated molecules in principle, can serve as a finger-print, which helps to recognize the type of material and possible conformations of molecular bonds in it. Therefore, inelastic light scattering can be considered as a useful instrument for detection of molecules active in the Raman mode by the specific spectral bands registered from the inelastically scattered light. It can be used for the detection of gases, liquid and solid analytes. Even very complex biological tissues, such as human blood or tissues can be analysed in order to establish cancer cells [1].

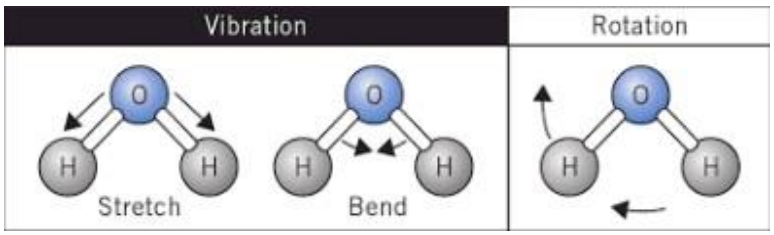

Fig.1 Vibrations and rotations in the water molecule.
The figure is reproduced from ref. [2].

Even though details of Raman scattering need the usage of quantum mechanical calculations, the main ideas can be illustrated qualitatively by a simplified scheme (Fig.2). The band of elastically scattered light (Rayleigh light scattering) can be depicted as the strongest one, illustrating that the main part of the light is scattered elastically. The Raman band with a lower

energy has much less intensity than the Rayleigh band and it has been named as the Stokes band. It can be detected experimentally by special separation of inelastically scattered light, which gave a small part of its energy to the molecular vibrations inside the investigated sample. The intensity of anti-Stokes Raman band is even lower than that of the Stokes band, because the probability of the process at which the energy is taken from the molecular vibrations and given to the incident light is the smallest. All these three processes can be schematically depicted on the language of virtual quantum states. Virtual means that the time during which a molecule can situate in this state is negligibly small in comparison to the time, which is usually typical for light absorption, fluorescence and phosphorescence processes.

On the topic of wave optics, Raman scattering can be represented as an appearance of overtone frequencies (bigger and smaller relatively to the frequency of the incident light) during the interaction of two oscillators: the light wave and the molecular oscillator. The scattered wavelength from the material will have three possible frequencies:

1. A first possibility is that there will be no change in frequncy.. A material molecule absorbs the photon energy, which goes to a virtual energy state, a very short-lived unobservable quantum state, and then back to the original energy level by scattering the same frequency as the excitation frequency $\nu_{o.}$ The interaction will result in an elastic Rayleigh scattering.
2. A second possibility is that the laser beam photons will give a part of their kinetic energy to material molecules when they interact with each other resulting in the changing of the material molecules into a virtual state. Then on to a vibrational level, which has a higher energy level than it had originally by scattering a frequency that was reduced to ν_o-ν_m. This type of shift in frequency is called the Stokes band.
3. A third possibility is that the energy of photons in laser beam was increased due to the interaction of the material molecules. That in turn will result in the molecules of the material going into a virtual state. Then back to an energy level, which is lower than it originally was, the frequency of scattered light was increased to ν_o+ν_m. This type of shift in frequency is called anti-Stokes shift.

The previously mentioned interactions are visualized in the following figure:

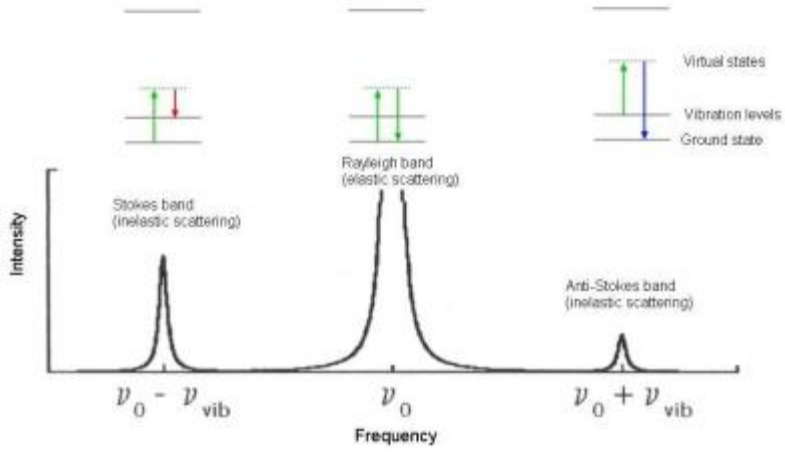

Fig.2 Spectrum of photon transition from the elemental ground level to the virtual states. The figure is reproduced from ref. [3].

As the Raman signal is usually quite weak there have been continuous improvements in Raman spectroscopy detection methods. Countless methods for sample preparation, illumination or scattered light detections have been created to enhance the Raman signal. In the following sub-chapters such methods will be introduced.

1.2 Coherent anti-Stokes Raman spectroscopy (CARS)

Coherent anti-Stokes Raman spectroscopy or in short CARS is also a "non-linear" Raman method [4]. In this method, multiple lasers, namely coherent lasers, are used to illuminate a sample. The frequency of one laser is constant and frequency of the second laser is tuned so that the frequency difference between the lasers is equivalent to a Raman-active frequency of the analyte molecule. Appropriate tuning can result in the effect that Raman frequency of the analyte molecule will be enhanced up to 5 orders in comparison with the conventional Raman signal [5].

In CARS, the process can be physically explained by using either a classical oscillator model or by using a quantum mechanical model that incorporates the energy levels of the material molecule. Considering that material molecules are like harmonic oscillators with characteristic frequencies of ν_m. The two laser beams with frequencies ν_1 and ν_2 ($\nu_2>\nu_1$) will interact coherently producing a strong scattered light with a frequency of $2\nu_1-\nu_2$. If the frequency

difference between the laser beams is equal to the characteristic frequency of the molecule then a strong light with a frequency of $\nu_1+\nu_m$ would be detected.

Strictly speaking for obtaining a strong Raman signal using two lasers one would need to tune them so that $\nu_2=\nu_1-\nu_m$. Then in the CARS regime the light with the frequency of $2\nu_1-\nu_2=\nu_1+\nu_m$ is detected (Fig. 3) and its intensity is several orders higher than the usual Raman light scattering. The frequency of this light $\nu_1+\nu_m$ is higher than ν_1, so in this sense, it is the Anti-Stokes type of frequency.

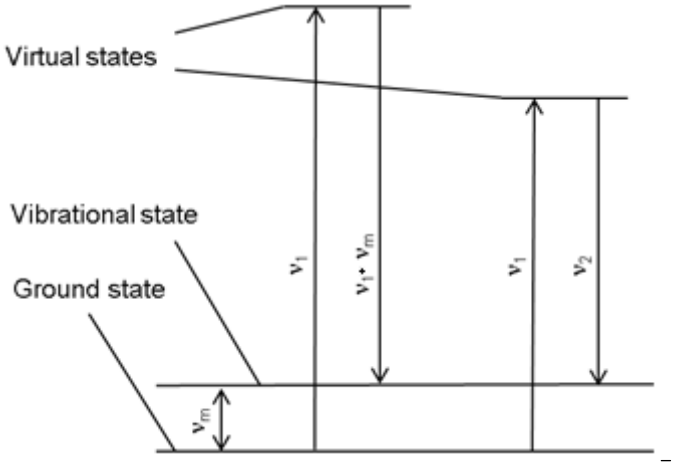

Fig.3 Transition scheme for CARS.

Scientific fields that use CARS are cell biology and tissue imaging. For cell imaging, fluorescence microscopy is usually used, but with CARS a label-free imaging is possible. CARS spectroscopy is also used in clinical applications and fast, video-rate imaging of tumour masses in healthy brain tissue [6].

1.3 Stimulated Raman spectroscopy (SRS)

If a sample is illuminated with a very strong laser pulse, a "non-linear" phenomenon would occur [7]. This means that compared to the continuous lasers with 10^4 V/cm^{-1} electric field if one would use pulsed lasers with 10^9 V/cm^{-1} electric field, a much larger part of incident light energy would be used in the Raman scattering. A very strong laser pulse with a 10^9 V/cm^{-1} electric field would transform up to half of its pulse energy to a coherent beam with Stokes frequency $\nu_0-\nu_m$ (Fig. 4). For an analogy of a continuous laser, only 0.001% would be used. This Stokes frequency is so strong that it acts like an additional illumination source and generates a second Stokes frequency of $\nu_0-2\nu_m$. The second one could act also as an additional illumination

source for the third Stokes frequency of ν_0-3ν_m and so on. This type of Stimulated Raman spectroscopy method would enhance Raman signal by 4-6 orders of magnitude [8].

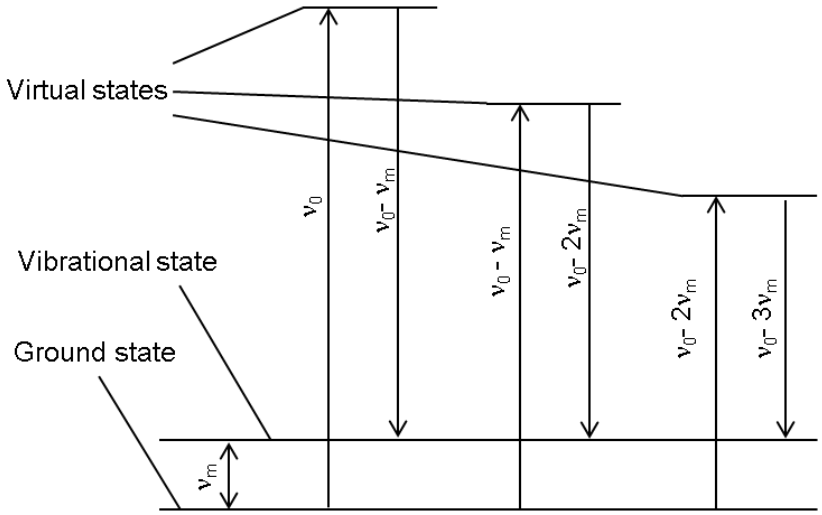

Fig.4 Stimulated Raman transition schemes.

Compared to the previous Raman enhancement method SRS provides background-free chemical imaging with improved image contrast that is essential for biomedical imaging. Just like CARS method, it can be used for label-free imaging [9]. In recent years it has even been used on plant tissues [10].

1.4 Resonant Raman spectroscopy (RRS)

Resonance Raman spectroscopy (RRS) is a Raman spectroscopy method in which the frequency of excited light is tuned so that it resonates or is near electronic transition inside the analyzed molecule. Such tuning has both benefits and drawbacks. The benefit is caused by a stronger light induced change in the molecular polarizability caused by mentioned electronic transition. It enhances the intensity of the Raman signal. However the drawback is that this electronic transition turns the molecule to the excited state from which it most probably will decay fluorescently. This fluorescence is overlapped with the Raman signal and complicates its detection and separation [11]. By applying this method, one could balance between the desirable benefit and the possible presence of parasitic fluorescence background. This is one of the main problems when UV lasers are used in the Raman spectroscopy.

Nonetheless, it has been found that in some circumstances the substance molecules can create a strong Raman scattering instead of fluorescence. This effect is also known as the

Resonance Raman. It happens when the illumination laser frequency is tuned in a way that crosses frequencies of electronic excited states and resonates with them. The amplitude of those resonated electronic excited states is enhanced up to 6 times in magnitude [12]. The supposed chromophoric group, which is accountable for the substance colour, inhibits the highest increase of enhancement. This is because the chromophoric group is accountable for the highest level of light absorbance. Highest intensity for the Resonance Raman comes from the frequencies that are equal to the primary electronic excited states (Fig.5). Therefore, excitation by means of a tunable laser is a key feature for application of the resonant Raman spectroscopy. Even if the laser frequency does not completely correspond to the exact value for primary electronic excited states, the enhancement of the signal can still be significant.

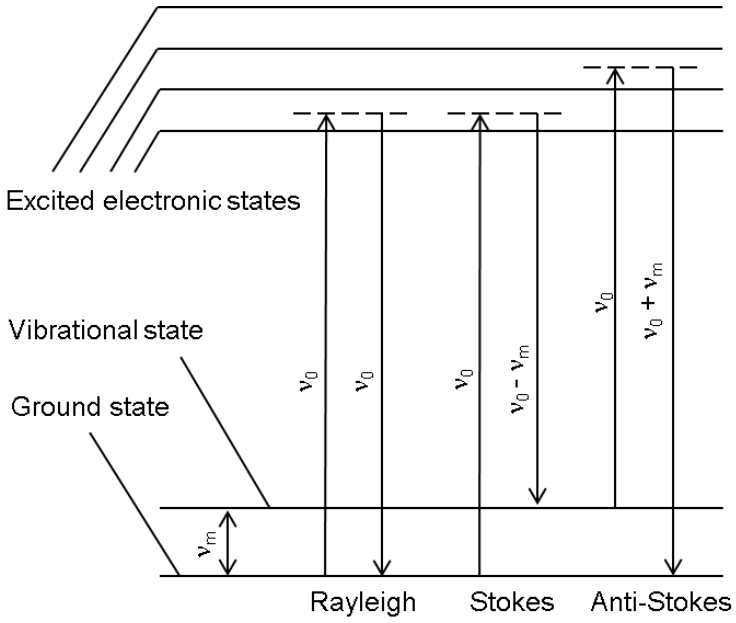

Fig.5 Transition scheme for RRS.

The main applications for RRS lie in the analysis of organic molecules. As mentioned earlier, the usual Raman spectroscopy signal is relatively weak to see specific molecule vibrations. For an example, RR spectroscopy has been used to study dioxygen molecule in Cytochrome-c-oxidase [13].

1.5 Surface-Enhanced Raman Spectroscopy (SERS)

Surface-Enhanced Raman Spectroscopy (SERS) is a method that exploits enhancement of Raman signal by the surface of the substrate. By placing molecules on certain metal surfaces, such as gold nanoparticles, one could increase the Raman signal of said molecules by up to 10 orders of magnitude [14]. There are two mechanisms behind the drastic enhancement for SERS,

both of which work simultaneously but are yet to be fully understood. This is due to the difficulties of looking for the enhancements separately. Considering that the Raman signal is proportional to the square of dipole moment ($P = \alpha E$) both enhancement mechanism influences can be viewed as such: one changes the polarizability (α) and the second changes the local electric field (E) near the analysed molecule.

Another way to understand the enhancement of SERS is by looking at the SERS intensity components [15].

$$I_{sers} = I_e N_{sur} \Omega A_e(\omega_e) A_S(\omega_S) \frac{d\sigma}{d\Omega}, \qquad (1)$$

where $A_e(\omega_e)$ and $A_S(\omega_S)$ are electromagnetic surface-averaged intensity enhancement factors, I_e excitation light intensity, N_{sur} is the number of adsorbed molecules excited by the light, Ω the solid angle of collection optics and $\frac{d\sigma}{d\Omega}$ the differential cross-section.

It follows that we have 3 possibilities for enhancement:

- The increase in the number of molecules that are on the metal surface compared to the smooth surface.
- The increase of the Raman cross-section.
- The increase of an electromagnetic surface averaged intensity enhancement factors.

Experiments have proved that by increasing the surface roughness the number of absorbed molecules was changed only a few times, leaving us with the last two possibilities. They are related to the model approximations named in literature as electromagnetic (EM) and chemical contributions to the enhancement of Raman signal.

EM model:

The main statements of the EM model are based on the properties of sub-microscopic roughnesses of the substrate. The nanostructure can be formed not only by the substrate itself, but also by specially deposited noble metal nanoparticles. These metal nanoparticles can interact with the exciting light because of special properties caused by their low dimensions (10-100 nm). The small size of the metal nanoparticles makes a special kind of light-induced electric polarization possible for their surface electrons. Collective oscillations of these electrons, driven by the alternative electric field of the light wave, are called surface plasma oscillations. Equality

between the frequency of photon, i.e. a quantum of light, and a quantum of plasma, i. e. the plasmon can be achieved for metal nanoparticles made of silver, gold and copper at certain frequencies of light belonging to the visible spectral range. A coincidence of frequencies for incident light and oscillations of surface plasma localized in the metal nanoparticles is called the localized surface plasmon resonance. A locally strong light-induced electric field of plasmons in metal nanoparticle causes the increase of $A_e(\omega_e)$ and $A_S(\omega_S)$ factors. It is because nanoparticles work as a kind of optical antenna redistributing and concentrating light energy in the vicinity of a nanoparticle. As a result, a cross- section of the light scattering processes, including Raman type of light scattering, can be much larger than the geometrical cross section of the metal nanoparticle.

The causes of such unusual properties of the surface electron oscillations in metal nanoparticles can be derived from the classical Drude model describing metal as a lattice of ions immersed into the "gas" consisting of the free electrons. It is known that metals shield the external static electric fields. It is because the external electric field charges metal by a way that its free electrons become displaced and their electric field completely compensates the external one. As a result theee external electrostatic field cannot create the electric field inside the metal. As a result, if electrostatic fields are applied to the metals, their dielectic permittivty is unclear. The dielectric permittivity shows how much the electric field inside a material differs from thattt of a vacuum.

However, free electrons cannot completely follow in time with the high frequency oscillations of the electric field inside the incident light wave. It creates a situation where at very high frequencies metal can pass the electric field from the incident light, i.e. behave as a dielectric. As an example of such behaviour the alkali metals in the ultraviolet light can be considered. The material reason for a high transparency of these metals in ultraviolet light is caused by the fact that they have a lot of free electrons. In reality electrons of such metals as aluminum, copper, gold, and silver are not completely free, but partially bounded. The degree of this bounding specifies different values of plasmonic frequency and different spectral widths of light induced plasmonic resonances for them.

Dielectric-like behavior of metals at high frequencies of incident light created the premises for definition of dielectric permittivity for the metals. It is defined as $\varepsilon_m = (1-(\omega_p/\omega)^2)$ for the ideal metal, which completely corresponds to the Drude model. Here ω is a frequency of incident light, ω_p is the volume plasma frequency. Frequency ω of surface plasmon in a small

spherical metal nanoparticle includes the frequency of the volume plasma ω_p and permittivity of surrounding dielectric:

$$\omega_{sp}=\omega_p/(1+2\varepsilon_d)^{1/2}. \quad (2)$$

Starting from the resonant equality of frequencies $\omega_{sp}=\omega$ and keeping in mind that $\varepsilon_m=(1-(\omega_p/\omega)^2)$ one can derive the equation for plasmon resonance conditions in which the relation between the dielectric permittivity of metal nanoparticles and the permittivity of the surrounding material is described as:

$$\varepsilon_m=-2\varepsilon_d. \quad (3)$$

As one can see, the permittivity of metal here should have a negative value. Physically it means only that the frequency of a light wave should not be very high in order to provide a situation where $(\omega_p/\omega)^2=3$ in the equation for the ε_m. Namely, it happens when the properties of a metal are still metallic, but close to the border between the metal and dielectric: permittivity is not so far from the positive values.

The consideration of light-induced electric fields near the small metal nanoparticle (Fig.7 and related equations) demonstrates that resonant condition $\varepsilon_m=-2\varepsilon_d$ stipulates the decrease of the denominator and as consequence increase the fraction describing the value of local electric field near the noble metal nanoparticle. This resonance condition similarly decreases denominators in the equation for the cross section of light scattering, and particularly Raman scattering, increasing its efficiency by several orders.

The above-mentioned description concerns only the case of dipole-type of light-induced charge distribution inside the nanoparticle. It is reasonable for nanoparticles with sizes up to several tens of nanometers. In case of bigger particles distribution of charges can be multipole. Analytically, it can be described as spherical particles by using the Mie theory of light scattering. Changing the shape of nanoparticles from spherical to elongated, it is possible to tune the spectral position of the surface of plasmonic resonance in such ranges, which are depicted in Fig. 6 for different metals.

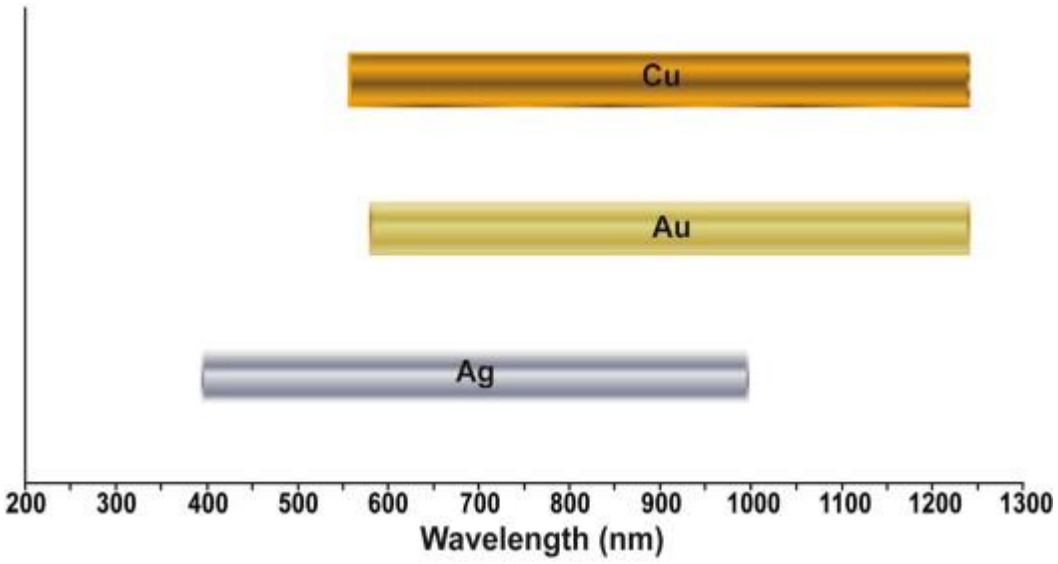

Fig.6 Approximate wavelength ranges where Ag, Au, and Cu have been well-characterized and are established to support SERS. The figure is reproduced from ref. [16].

Below, a short calculation demonstrates the collective oscillation if a spherical metal nanoparticle is excited by a light beam:

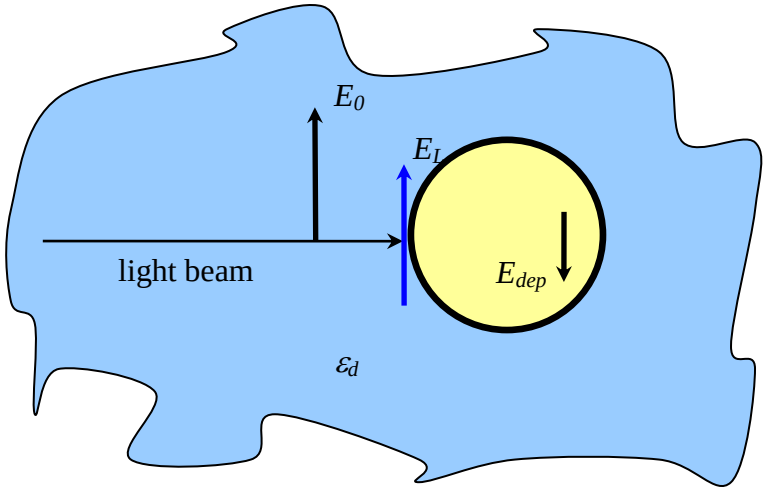

Fig.7 The scheme of electric fields acting on the metal nanoparticle: E_0 – the electric field of incident light, E_{dep} – depolarization field, E_L – resultant local electric field, ε_d – permittivity of the neighbouring dielectric.

Resulting local electric field E_L acting on the particle will consist of the incident electric field E_0 and the depolarization field E_{dep} caused by the polarisation of the nanoparticle atoms. If the particle is situated in the medium with permittivity ε_d, the equation for the local field is:

$$E_L = \frac{E_0}{\varepsilon_d} + E_{dep}. \tag{4}$$

The differential element of the depolarization of the electric strength dE_{dep} can be represented according to the Gauss's theorem by the sum of charges enveloped by the element dS of nanoparticle's surface:

$$dE_{dep} = \frac{P\cos(\theta)dS}{4\pi\varepsilon_0 r^2}, \tag{5}$$

where θ stands for the angle between the normal to the unit surface area dS and the polarisation direction P and r is the radius of the particle.

$$E_{dep} = \int_0^{\pi} \frac{P\cos(\theta)dS}{4\pi\varepsilon_0 r^2} 2\pi r\sin(\theta)d\theta = \frac{P}{3\varepsilon_0}. \tag{6}$$

We shall set a minus sign before the value obtained in equation (16). It is because the depolarization field is directed opposite to the incident field, so for the resultant local field:

$$E_L = \frac{E_0}{\varepsilon_d} - \frac{P}{3\varepsilon_0}. \tag{7}$$

Polarisation P of the particle can be represented by the use of the dielectric susceptibility χ:

$$P = \varepsilon_0 \chi E_L, \tag{8}$$

where

$$\chi = (\frac{\varepsilon'}{\varepsilon_d} - 1). \tag{9}$$

Substitution of (9) and (8) into (7) finally resulted in:

$$E_L = \frac{3}{2\varepsilon_d + \varepsilon'} E_0. \tag{10}$$

One can see that the denominator of this fraction is close to zero, when

$$\varepsilon' = -2\varepsilon_d. \tag{11}$$

Such a resonance condition causes stronger enhancement of the local electric field E_L near the nanoparticle, which increased $A_e(\omega_e)$ and $A_S(\omega_S)$ factors and thus the SERS signal itself.

Chemical model:

The chemical contribution into the enhancement of Raman signal could not be separated from the electromagnetic signal until the recent times by devising nanoengineering methods for manipulation of plasmonic substrates [17]. This contribution is called chemical because of its realization that the analyte molecule should be placed very close to the surface of the nanostructured metal. The distance should be small to provide the possibility of the transfer of electrons from the substrate to the analyte molecule by such a way, that this electron could become common both for the substrate and for the contacting with its analyte molecule. This creates a kind of a weak chemical bond between the substrate and the analyte which is why it is named as a chemical contribution. Here, the transfer of certain separated electrons is considered in contrast to the former case, where the collective electronic oscillations were considered. In the previous case electrons were not transferred but situated inside the metal nanoparticle. These features highlight the difference between the transfers of separated electrons from collective plasmonic effect. However, in this case, the analytes deposited on noble metals both effect to give enhancement of the Raman signal in the same spectral range. Therefore, it is hard to study them independently.

The transfer of an electron from the substrate to the analyte molecule can also cause the change in the molecular polarizability:

$$\frac{d\sigma}{d\Omega} \approx \alpha^2 \tag{12}$$

The polarizability itself is proportional to the two following values.

$$\alpha \approx \left(\frac{1}{(E_i - E_j) - h\omega + i\Gamma} - \frac{1}{(E_i - E_f) + h\omega + i\Gamma} \right) \tag{13}$$

Where E_i, E_j and E_f are energies depicting the initial, intermediate and final stage of the molecule. If the energy of the exciting light $h\omega$ is chosen to be equal to $E_i - E_j$ then polarizability α will increase rapidly and resonance would occur. Even if the resonance is not fulfilled for the molecules not on the metal surface, resonance could still happen. The resonance can be further appraised as a result of two enhancement factors:

$$A_{chem} = A_{CT} A_{AS}, \tag{14}$$

Where A_{CT} is the value which corresponds to a charge transfer mechanism that is linked to electron transitions from Fermi states of the metal to unoccupied states of the adsorbed molecule or the molecule occupied states to the Fermi states of the metal (Fig.8). This charge transfer is tuneable with the exciting light. By having its energy value close to the former or later mentioned condition, the second value A_{AS} corresponds to the active state mechanism, which occurs on a smaller scale where there would be a surface roughness on the atomic scale. These roughness discrepancies called "active sites" create the additional possibilities for electron transitions (Fig.8). Chemical model enhancement has been noted to be 2 orders of magnitude higher signal than the usual Raman signal [18].

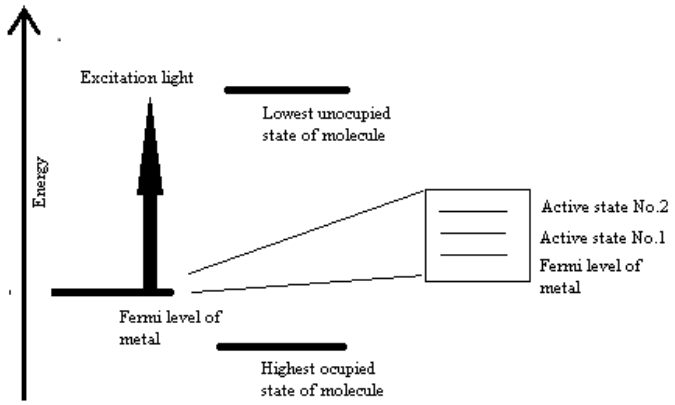

Fig.8 Energy scheme of metal with additional atomic roughness and molecule with its highest unoccupied and lowest occupied state.

The downside of SERS is the difficulty of its spectral interpretation. The enhancement is so drastic that Raman frequencies that are weak in usual Raman spectroscopy can appear in SERS. Even if there are contaminations in the sample there will be additional peaks. However, because of the chemical interactions on the metal surface, some of the frequencies might be quenched. Having multiple factors that change the signal of the interpretation of SERS makes it difficult to use. Thus, for example, SERRS spectroscopy, Surface-Enhanced Raman Resonance Spectroscopy, was devised. Using this signal enhancement compared to usual Raman is up to 10^{14} orders in magnitude. But the biggest benefit here would be that SERRS spectra are similar to RR spectra which are easier to read. SERS itself has found use in many different applications such as biosensors, chemical warfare agents, and single molecule detection [18].

1.6 The aim of this study is using Graphene-Enhanced Raman Spectroscopy (GERS) for detection of adenine biological molecule

Recently it was revealed that not only nanostructured noble metals, but also graphene can provide enhanced Raman signals for the molecules deposited on it. Since plasmon resonance for graphene is observed in the deep infrared spectral range and enhancement of the Raman signal was detected for the excitation of samples by visible laser light, one can conclude that this enhancement is caused by a purely chemical contribution separated from the electromagnetic contribution. This is due to the unique properties of the chemical contribution of graphene to the SERS effect that can be separated from the electromagnetic one and has to be studied independently.

The purpose of this work is the detection and investigation of graphene enhanced Raman scattering from the biologically important molecules, such as DNA constituents. Particularly, here the GERS effect is studied on the example of one of the DNA constituents named adenine. Since the chemical conformations of DNA and its constituents accompany certain diseases, detection of such DNA constituents as adenine and its possible conformations can be potentially important for biological and medical diagnostics of these diseases [19].

Some data about graphene and its properties finish this introductory part. This data will be suitable during further consideration of graphene enhanced Raman scattering.

Graphene is a 2D atomical crystal, consisting of carbon atoms in a hexagonal lattice structure (Fig.9). But graphene has not been received experimentally for a long time. Until 2004 a simple method was devised to create single graphene layers [20]. This method made it possible to start using graphene-enhanced Raman spectroscopy (GERS).While studying graphene, researchers had found many interesting facts about this material. Such as 2.3% of the optical light passing it [21] and the appearance of plasmon resonance in the THz range [22].

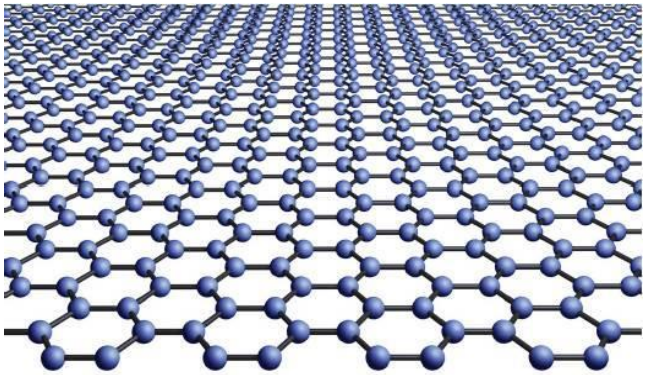

Fig.9 Graphene crystal structure.

Graphene, as an additional part of our system, is a multifunctional improving agent, having many positive effects. For example: acting as a suppressor to exclude interactions of noble metals (Fig.10), internal label due to its atomic uniformity, chemical inertness and clean Raman signal of graphene and acting as a fluorescent light quencher. In some cases, the signal amplitude having a fluorescence signal might decrease the Raman signal amplitude but the sensitivity of the molecule will be still high [23].Though the main positive aspect why GERS is useful as a Raman spectroscopy method is because it behaves like SERS method without the EM mode.

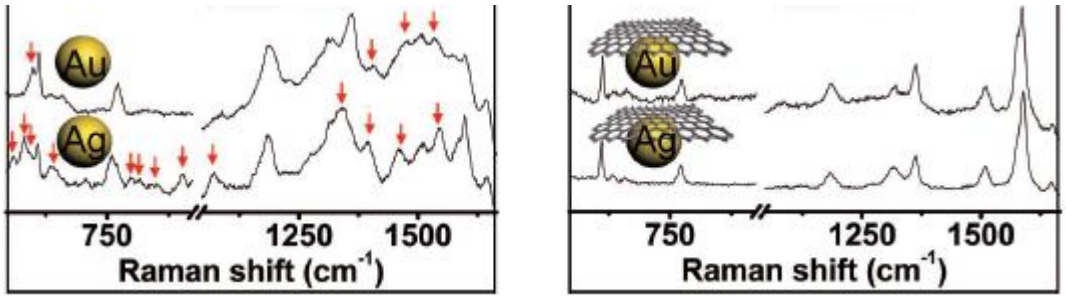

Fig.10 Surface passivation of the metal substrate for SERS with the addition of graphene. (a) Usual SERS with the Au and Ag nanoparticle-molecule interactions and (b) Graphene-shell isolated SERS. Au and Ag different SERS features of R6G marked with arrows. The figure is reproduced from ref. [24].

SERS as a method for characterisation brought major developments to material science. It is a method to study materials for further technological advancements. The same could be said for GERS but being able to use graphene with SERS, as seen in Fig.10, it has gained even more interest.

2. Materials and methods

Materials:

Silver nanoparticles (Ag NPs), which were used in our experiments, were made by Alexey Treshchalov with the same procedure as in reference [25]. Where he used He +5% H_2 +1% N_2 plasma jet treatment for the synthesis of surfactant-free Ag NPs with a narrow size distribution: 12-22nm as seen in Fig.11 insert. The initial amount of silver nitrate from which the NPs were obtained is 0.1mM.

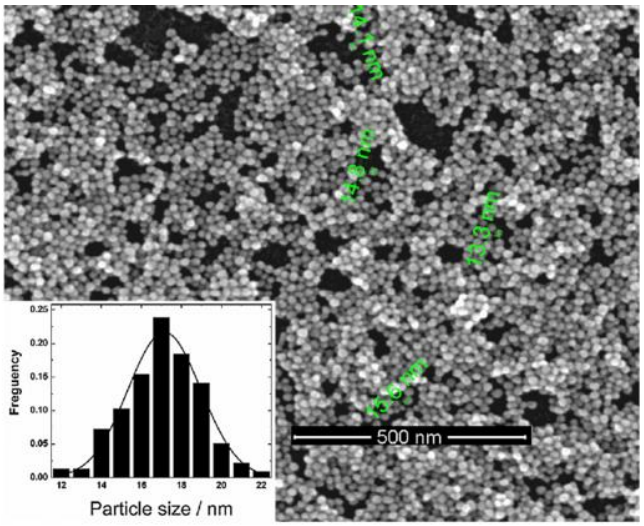

Fig.11 SEM image of Ag NPs deposited onto GC surface by vacuum-drying technique. The insert shows the size distribution of NPs. The figure is reproduced from ref. [25].

Gilded silica-gold nanoparticles (Si-Au NPs), which were used in the experiments, were prepared by covering the silica core NPs with gold seeds. The silica core NPs were prepared by the Ströber method [26] and then functionalized by amino groups that made the surface negatively charged. This provided a good coverage of silica core by the gold seeds that were positively charged. By the charge neutralisation, the gold seeds joined together to form a continuous gold shell consisting of the connected gold islands around the silica core [27]. Gilded NPs dispersed in water were obtained. The size distribution of the NPs that included silicone was around 200-250nm in diameter with a gold shell thickness of approximately 15-20nm (Fig.12). The concentration of the particles is estimated to be ~10^9 particles per cm^3.

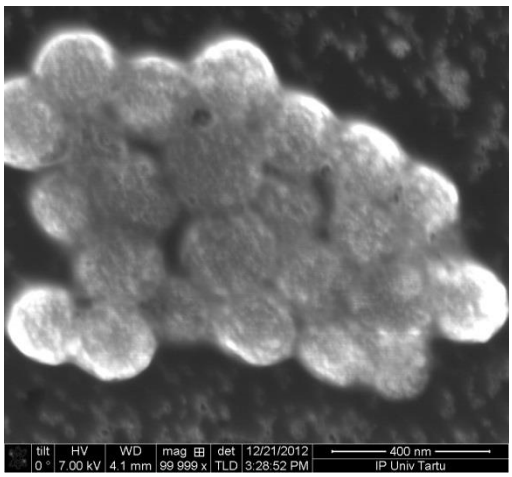

Fig.12. SEM image of gilded nanoparticles settled on the silicon substrate.

The graphene used in the experiments was made by the company Graphene Square. It was prepared by the chemical vapour deposition and transferred on a silicon substrate with a 200nm thick silica layer.

The molecule for the detection in the modified Raman spectroscopy setups was adenine. Adenine is a chemical component of DNA molecule [28] with a relatively weak fluorescent signal. Thus for small concentrations, instead of fluorescence detection, Raman technique would be more efficient. In this case, adenine was diluted in water to have 0.1 mg per ml concentration. Having a good detection for adenine could open new prospects for biomedical analysis. The idea is to have both healthy and unhealthy cells which can have different arrangements of such biological molecules as adenine. It is important not only to detect adenine itself but to see how it changes by the means of monitoring changes in the Raman spectra.

Methods:

The bright-field microscopy method, which was used in our experiments, was done with an Olympus BX50 microscope. It consists mainly of four main parts: a light source, such as a lamp, a condenser lens, that focuses light on the sample, an objective lens, which collects light from the sample and a detector to view the image as seen in Fig.13a. The typical appearance of a bright-field microscopy image is a dark sample on a bright background, hence the name. Bright-field itself is the most known illumination method. Additionally, to extract light bulb filaments Köhler illumination, an extremely even illumination of the sample should be used.

For switching to dark-field microscopy method, the light source was switched off and a new light source was placed around 135 degrees to the sample at a normal angle. This was done because in dark-field microscopy, a light source needs to be focused from the sides to the sample so that only scattered light from the sample reaches the objective lens. This produces the classical appearance of a dark background with bright objects in the image. A simple design for the usual dark-field microscopy method can be seen in Fig.13b. Compared to the previous method dark-field spectroscopy used to enhance the contrast of images of unstained and uncolored objects. Making it well suited to observe transparent unstained biological samples.

Both mentioned methods have limitations. The samples must be strongly illuminated to get a clear image. Adversely, this can cause damage to the sample so the illuminations must be done with utmost care. Most of the samples, like cells, are quite transparent, thus for these methods staining the sample might be needed. This will introduce extraneous details into the sample that should not be present. By comparison, the images in both methods seem opposite to each other, however, different features are visible in each. In the former method, the features will be visible where the shadow is cast on the surface by incident light or because the surface is less reflective, possibly from the scratches. Features that might be too smooth to cast shadows will not appear in bright-field, but by side illumination such as in dark-field, they become visible.

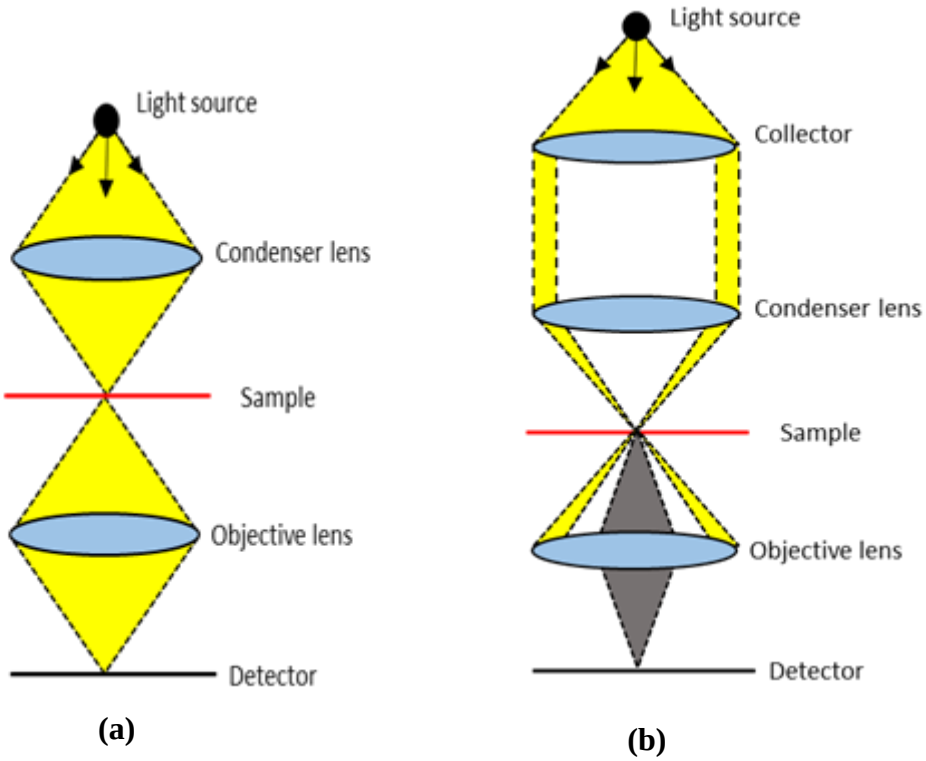

Fig.13 Basic design of (a) dark-field and (b) bright-field illumination.

The previous methods were used to see the adenine and NPs solution droplets visually. For actual size measurements of the NPs, they were observed with Zeiss EVO MA15 low vacuum scanning electron microscope (SEM). The main components of SEM are an electron source, an anode, electromagnetic lenses and an electron detector. Instead of light, an electron beam is being used, based on the dualism principle. The electron beam is accelerated and focused on a sample by the lenses. The sample emits secondary electrons which are then detected (Fig.14). The number of secondary electrons depends on variations of the sample surface. By scanning the beam and detecting the variation of the secondary electron amount, one can create an image of the sample surface. The electron beam can also ionise the atoms thus emitting X-rays, which depends on the elementary structure of the sample. By scanning once again both previously mentioned channels one can deduce the chemical nature of the sample and topography. Other types of interactions between the beam and the surface would allow for various analyses to be conducted. Thus, SEM microscopy mode allows one to obtain a magnified image of the surface of thick samples to analyse their structure.

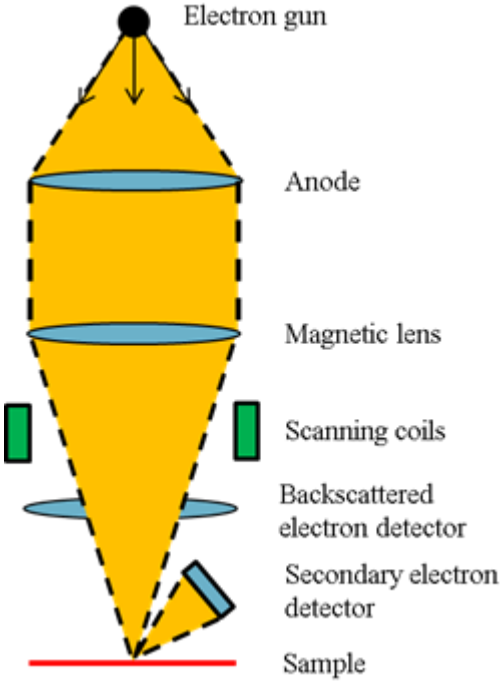

Fig.14 Basic design of SEM.

For Raman measurements, the Renishaw in Via micro-Raman microscope was used. In the case of Raman spectroscopy, there are six main components. Monochromatic light source, such as a laser, that illuminates the sample. From the sample, the light will be scattered and passed through a high-efficiency laser line rejection filter, such as a notch filter. From there, it enters a spectrometer with a single slit. From the slit, the light enters a diffraction grating and

finally the CCD camera. The light which was scattered from the sample will be composed of inelastic and elastic scattering. The scattering detected by the CCD camera will give respectively Stokes or anti-Stokes bands and Rayleigh bands as seen in Fig.15. Different frequency peaks from the Stokes bands correspond to the different sample molecule vibrations. By knowing which vibration frequencies correspond to which molecule, it is possible to identify which molecules there are in the sample.

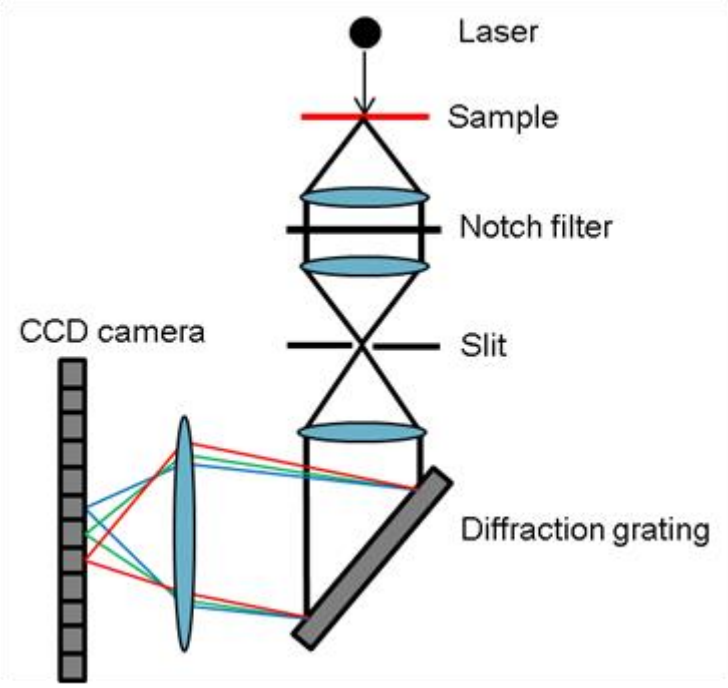

Fig.15 Basic design of Raman microscope.

3. Microstructure of drop deposited samples

Experimental results of SERS were obtained for the adenine material dissolved in water and drop-casted and dried on the graphene and several other substrates, such as glass, quartz, silicon and the same substrates with preliminary deposited gold and silver nanoparticles. These substrates were taken as reference substrates allowing to compare the electromagnetic and chemical contributions to SERS.

The experiments testified that direct mixing of water solutions of adenine with a noble metal, particularly silver nanoparticles, can result in chemical interaction and a change of adenine molecular conformation. Particularly adenine molecules can form a kind of circular structures clearly visible in the optical microscope (Fig.16). These structures testify that a nanosized noble metal can change the chemical conformation of the adenine molecules. Such circular membrane-like structures were observed by other scientific groups as well [29]. To minimize the influence of a noble metal on the conformation of the adenine molecule, it was decided not to use the water based solutions, in which adenine and the noble metal nanoparticles are initially mixed together, but to firstly deposit the noble metal nanoparticles and then put the adenine on the top of them. Glass and silicon substrates with preliminary deposited Au-SiO_2 and the silver nanoparticles were taken as surfaces for comparison. Depositions of the nanoparticles were also done by means of their drop-casting from water dispersions. The peculiarities of microstructures obtained for deposited droplets are described in this section.

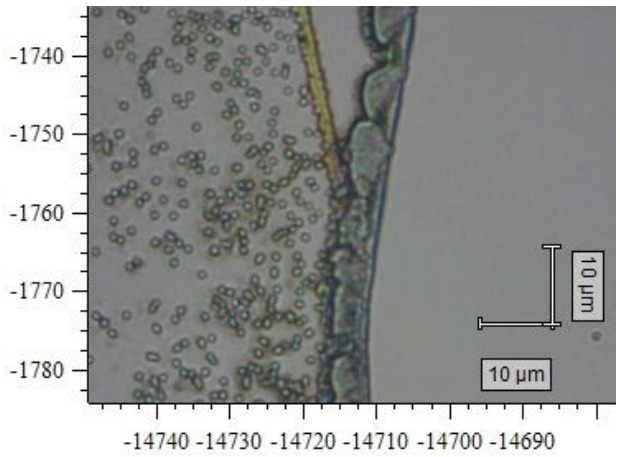

Fig.16 Microscopic picture of the adenine mixing with gold solution droplet on graphene.

3.1 Usage of drop coating for deposition of metal nanoparticles

Special nanoparticles consisting of 200-nm-silica core and covered by ~20 nm gold seeds were prepared and dispersed in water. Selection of such certain nanoparticles was done because of several reasons. Small single nanoparticles with sizes in the ranges of several nanometers work more as light absorbers. Bigger silica cores, on the one hand, can provide more contribution to the light scattering and as a part of it to Raman scattering. On the other hand, close placement of gold seeds on the surface of the silica cores can result in the interaction of plasmons induced in neighboring seeds. The local plasmonic field can be enhanced several times by this interaction and the so-called plasmonic and Raman hot spots can be formed between the gold seeds covering one silica core. This idea obtained experimental confirmation in one of the papers published by N. Halas group [30]. In this study, the comparison of SERS enhancements was done by the complete and incomplete gold shells formed around the SiO_2 core. It was concluded that the incomplete gold shell near the silica core indeed can provide stronger Raman signal from contacting an analyte than a continuous gold shell.

Prepared water dispersions of Au-SiO_2 particles had a distinctive bluish color (Fig.17, left part). Visually, it explains the plasmonic properties of such finely dispersed gold. It is known that dispersions of gold nanoparticles with sizes in the range of nanometer units have red color in transmitted light. This characteristic feature was noted in early times by M. Faraday, who was one of the first scientists, who started systematic investigation of metal colloids [31]. The red color in transmittance is present, because bluish and greenish tints are absorbed and scattered. It is because dipole plasmonic resonance for gold causes such light absorption and scattering is situated in the greenish spectral range near 520 nm.

Fig.17 Image of nanoparticle dispersions in water: (left) gold-covered nanoparticles, (right) silver nanoparticles.

Bigger particles have a contribution to light extinction from higher light-induced multipoles. These multipoles cause broadening of resonance in light extinction mode, so more reddish colors had started to be absorbed and scattered. That is why the color in transmitted light for dispersion of bigger gold particles becomes more bluish.

A droplet of such bluish water dispersion of Au-SiO_2 nanoparticles was carefully studied under the microscope. The fact that the cross section of light scattering from Au-SiO_2 nanoparticles is higher than their geometrical cross section, allowed us to trace the position of the nanoparticles by the optical microscope in the dark-field light scattering mode. They were visible as bluish-greenish bright spots on the dark background (Fig.18b). The Small size of the nanoparticles allowed observation of their Brownian motion in water. At the same time there was also directional movement of nanoparticles in radial directions from the center to the edges of the droplet. As a result of evaporation at room temperature, most of the nanoparticles that were collected formed a ring trace of the initial size of the droplet (Fig.18). This so–called "effect of coffee rings" formed after the drying of droplets wereas described earlier in ref. [32]. The evaporation of liquid from the surface of the droplet results in a lack of molecules. To replenish it, the flow of liquid and accompanying nanoparticles from the center to the edges of the droplet is formed. Since SERS-active sites are formed usually at the areas, where noble metal nanoparticles are collected quite densely, the mentioned rings made of self-assembled nanoparticles can be taken as SERS-active substrates.

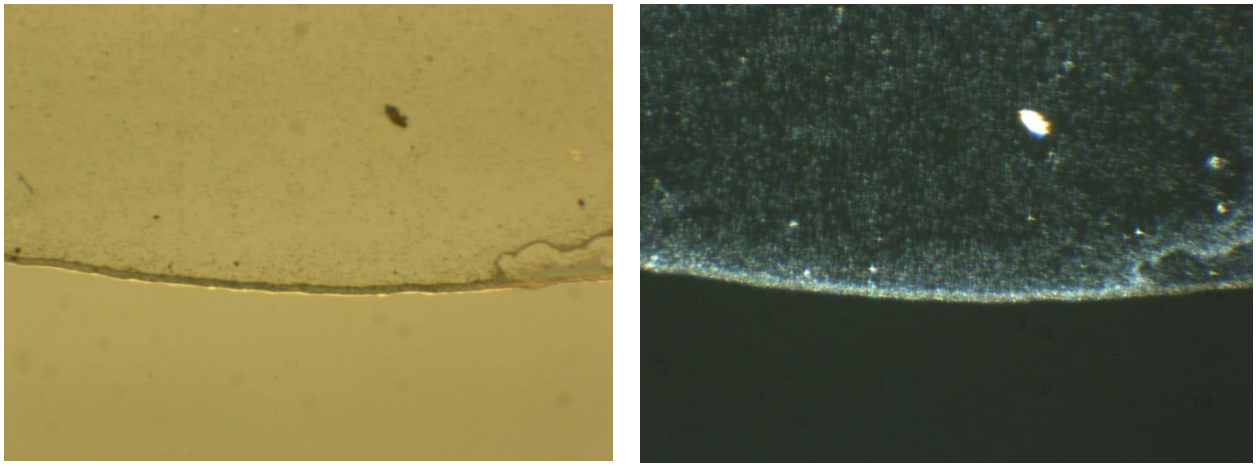

Fig.18 Microscopic picture of gold-covered nanoparticles dispersed in water and dried on a silicon substrate at room conditions: (a) bright-field image, (b) dark-field image.

Some authors also reported the use of fractal-like aggregates of the noble metal nanoparticles as SERS-active surfaces [33, 34]. In that case, aggregates of nanoparticles form a

branched network, the nodes of which served as Raman hot spots. A similar branched structure was obtained as a result of quick drying of the nanoparticles' dispersions on the hot stage at the elevated temperature ~100^{o}C (Fig.19). One can see that nanoparticles did not have time to migrate to the edge of the droplet in the event of quick drying of the liquid. The boiling process teared the surface layer of liquid together with particles. As a result, radially branched distribution of nanoparticles was formed on the silicon surface (Fig.19). The experiment testified that hot spots in the obtained structure are randomly distributed and can seldom be found. Therefore there were no further experiments with this network of nanoparticles.

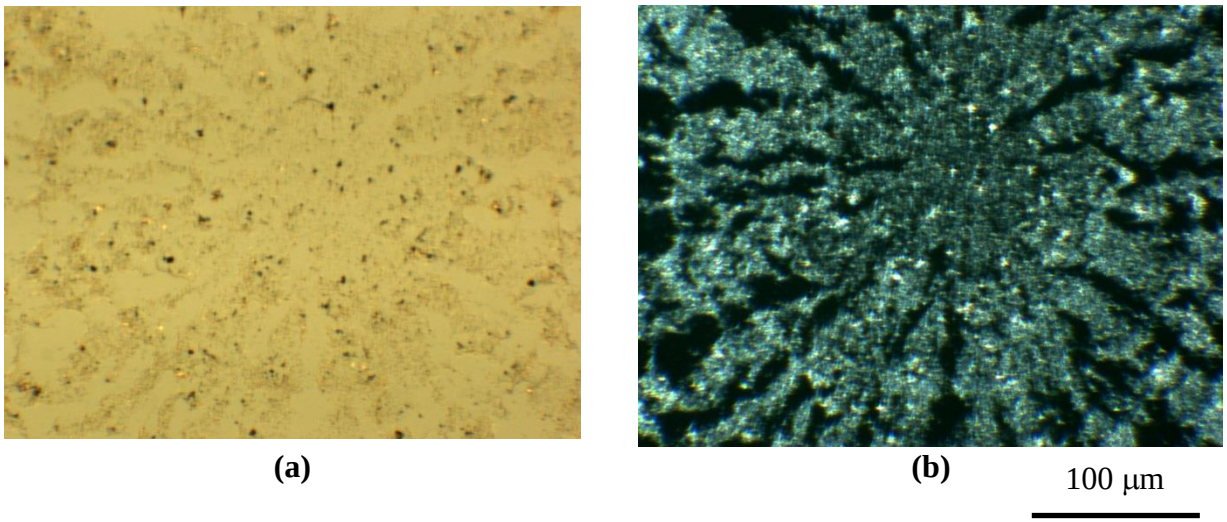

Fig.19 Microscopic picture of gold-covered nanoparticles dispersed in water and rapidly dried on the silicon substrate at 100°C: (a) bright-field image, (b) dark-field image.

As a variant of the preparation of a SERS-active surface, the collection of nanoparticles was considered at the interface of two unmixing liquids with their further deposition on the hydrophilic glass substrate by means of deep coating [35]. This process was realized by the addition of several milliliters of hexane to the bottle with water dispersion of the Au-SiO_2 nanoparticles. Since the density of hexane is smaller than the density of water, hexane was arranged finally as a top layer. As a further addition, several droplets of acetonitrile were added to the bottle that resulted in the collection of Au-SiO_2 nanoparticles at the hexane-water interface. When the hydrophilic glass slab touched the liquid interface with the nanoparticles, they were partially stuck to the glass slab. After carefully pulling the glass slab from the bottle, it appeared that several fragments of the nanoparticle layers had deposited on the glass. Even after completing the process very carefully, the top hexane layer essentially washed out nanoparticles

from the glass during the removal. Remaining nanoparticles showed weak adhesion to the glass surface. Therefore, this method was not used in most experiments.

Dried droplets of silver dispersion demonstrated the same collection of nanoparticles on the edge of the droplet (Fig.20). The silver nanoparticles themselves looked like a yellowish bright spots in the dark-field spectroscopy mode. This color is specific for the small spherical silver nanoparticles having sizes of several tens of nanometers. Dipole plasmonic resonance for them has a maximum near 400 nm. Plasmonically, silver could be more beneficial than gold, because it has narrower spectral band of resonance, which means that the thermal damping of plasmon oscillations is smaller [36]. However, silver suffers from the oxidation [37]. This fact usually limits SERS applications of silver, because even very thin oxide layer on the silver surface can essentially decrease an electromagnetic contribution to the SERS effect. Since there are silver colored spots in the dark-field images, the plasmonic properties of the silver coating are in effect. So, in the following section 4 some SERS data obtained on them are demonstrated.

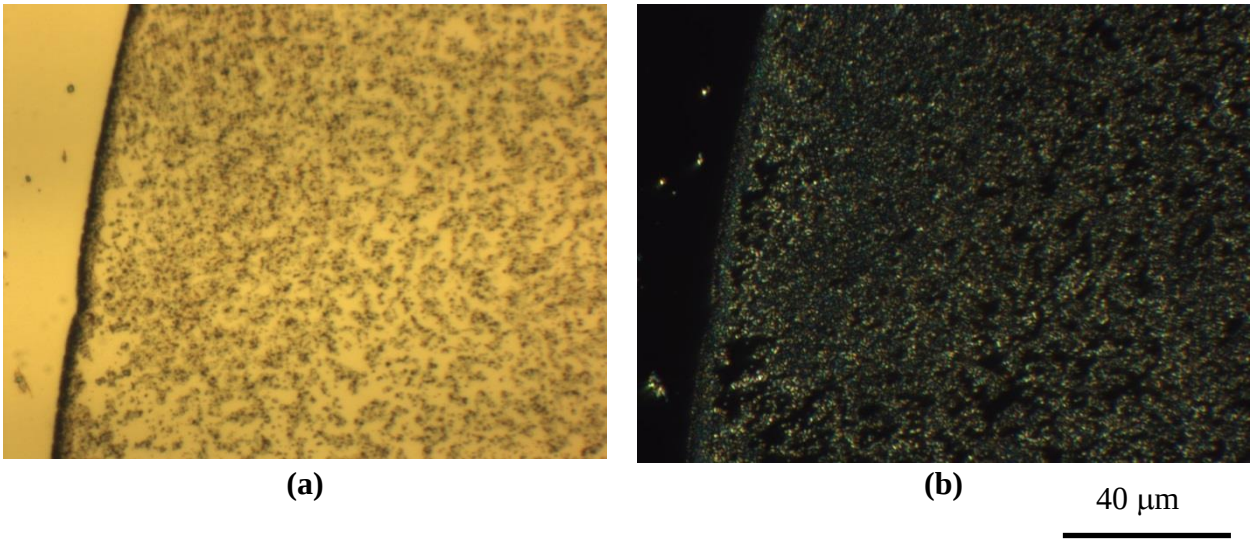

Fig.20 Microscopic picture of silver dispersed in water and dried on silicon substrate at room conditions: (a) bright-field image, (b) dark-field image.

3.2 Adenine droplets on hydrophilic and hydrophobic surfaces

Structures formed after drying of the adenine water solution depend on the concentration of adenine in the water. Initially, a concentration of 1 mg of adenine in the 1 ml of water was prepared. The drying of this solution showed that after the evaporation of water, adenine forms quite evident crystalline structures (Fig.21). It is worth to note that a droplet of liquid containing a dissolved material, which can be crystallized, comes in competition with the “coffee ring effects” [38, 39]. At such high concentrations, as in the case of this study, crystallization prevails

over the collection of material on the edge of the droplet, therefore the “coffee rings” are not very evident. Crystallization of the material is undesirable for this effect because the deposited material has a non-uniform thickness and the enhancement of the Raman signal can be caused not by SERS effect itself, but simply by increasing the thickness of the measured sample’s area.

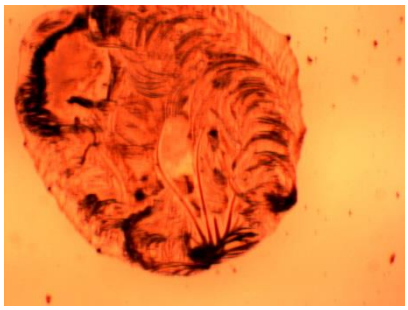

Fig.21 Crystallized droplet of adenine on the graphene surface.

In order to obtain a less pronounced crystallization and a more uniform sample thickness, initial adenine solution was 10 times diluted. The dried structures became more homogeneous in thickness, but on hydrophilic surfaces, the “coffee ring effect” became more evident. It was decided to use hydrophobic silicon substrates instead of hydrophilic glass. Having a lesser tendency to spread, the dissolved material was concentrated inside the droplet almost until its complete evaporation [40]. As a result, instead of the “coffee ring” , the adenine material forms a hydrophobic, almost a circular shaped film with more homogeneous thickness. Despite the fact that the “coffee ring effect” cannot be completely avoided, it is not excessively pronounced with this method (Fig.22).

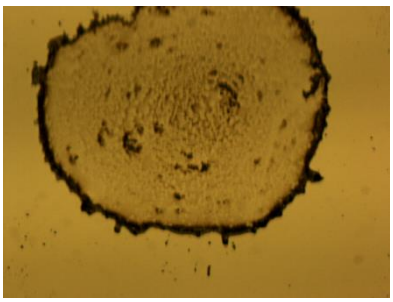

Fig.22 Adenine droplet dried on graphene.

Since graphene surface is hydrophobic, the above-mentioned approach was applied for the deposition of droplets of the dissolved adenine solution on the graphene based on the SiO_2-Si substrate. These samples were compared with adenine droplets dried on the top of the rings

formed by the noble metal nanoparticles described above. Investigation of the intersection points of two dried droplets (Fig.23) allows to compare SERS signals detected from them with Raman signals measured on the border of the droplets, but far from the intersection. By such a way it is possible to measure and compare the Raman signal from the sample areas having similar thickness without and with the influence of the noble metal nanoparticles placed in the underlying layer.

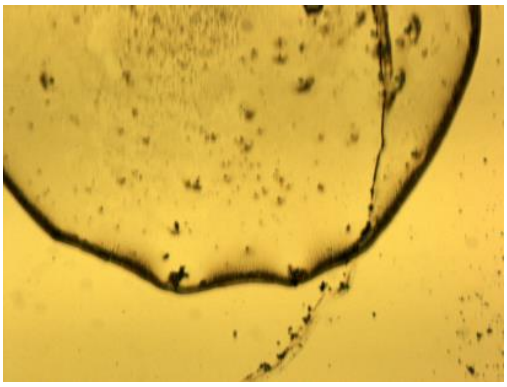

Fig.23 Intersection: the adenine droplet is partially overlapped with the initially deposited silver colloid.

4. Raman spectra of adenine in GERS

Raman spectra of used substrates were initially measured to distinguish the Raman bands of substrates from the Raman bands of the adenine. The Raman spectrum of the silica substrate (Fig. 25, spectrum 1) is determined by known SiO_2 vibrations, which are described, for example, in references [41-44]. The most pronounced band at 430 cm^{-1} is originated from the oxygen atom vibrations with identical distortions of neighboring Si-O bonds [41], i.e. symmetric stretching vibrations [42]. The band at 800 cm^{-1} is also associated with symmetric stretch vibrations of the oxygen atoms, but these vibrations involve also a substantial amount of surrounding Si atoms. The small peaks at 485 and 600 cm^{-1} are associated with defects in the silica lattice. These defects are due to the formation of 4-membered (4 oxygen atoms in the ring) and 3-membered (3 oxygen atoms in the ring) rings with vibrations at 485 and 600 cm^{-1} respectively [43]. The bands at 1056 and 1205 cm^{-1} (Fig.24, spectrum 1) are similar to those associated with Si-O transverse and longitudinal optical modes [44].

Silicon has Raman bands at 520 cm^{-1} and in the range of 950–1000 cm^{-1} (Fig.24, spectrum 2). These bands can be assigned with the first- and second-order Raman scattering from the optical phonons of Si lattice [45, 46]. Graphene deposited on the Si/SiO_2 substrate has typical Raman bands [47] at 1580 cm^{-1} (so-called G band) and at 2700 cm^{-1} (so-called 2D band) (Fig. 24, spectrum 3). The absence of the defect related band testifies that our sample is one layer of graphene and the number of defects in it is negligible.

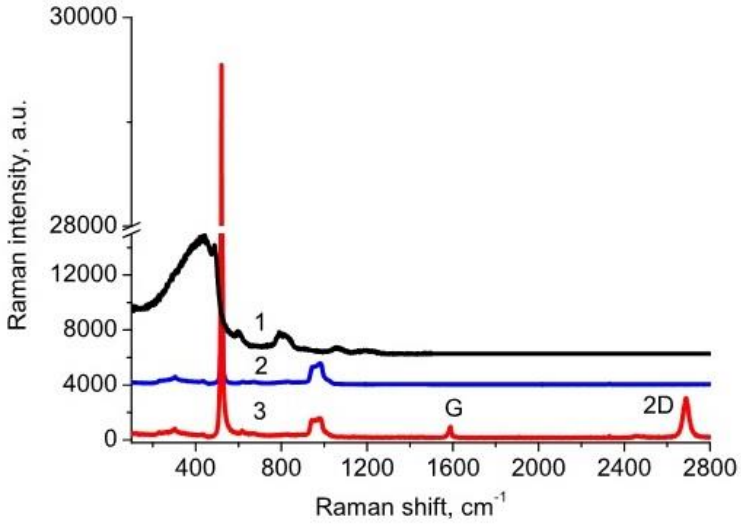

Fig.24 The Raman spectra of silica (1), silicon (2), and graphene on silicon (3). The spectra is not normalized but only shifted along the vertical axis to clarity.

Knowing the Raman bands of the substrates, it is possible to distinguish them from the Raman bands of the adenine material (Fig.25, spectra 2 and 3). Together with the adenine bands, there is a 2D band of graphene and silicon bands at 520 cm^{-1} in the range 950–1000 cm^{-1} (Fig.25, spectrum 1). Adenine spectra 1 and 2 are tilted in relation to the horizontal axis because of the presence of parasitic fluorescent background from adenine. This background is less pronounced for the adenine deposited on the graphene layer because graphene is known as a quencher for background fluorescence [48, 49]. Some Raman bands of adenine are overlapped with the G band of graphene; therefore graphene Raman spectrum is hardly distinguishable from the overlying adenine. The correlation of adenine Raman bands with its molecular vibrations can be found in literature, for example in ref. [50]. The spectral position of Raman bands for adenine measured in the experiments is well corresponding to the data from literature.

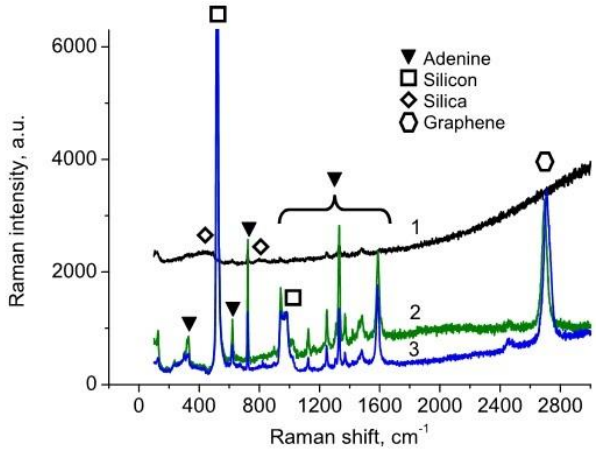

Fig.25 Raman spectra of dried adenine droplets deposited on quartz (1) and graphene (2, 3). Excitation wavelengths used are 514 nm (for spectra 1 and 2) and 488 nm (for spectrum 3). The spectra is not normalized but only shifted along the vertical axis to clarity.

At the same time, adenine demonstrates a signal up to 12 times stronger in case of deposition of graphene substrate in comparison with the one, which was deposited on quartz. As discussed earlier, such enhancement can be caused only by chemical contribution to the Raman signal. The precondition for such contribution should involve a close placement of adenine and graphene. Undeniably it can be so that the benzene ring of adenine becomes overlapped with the carbon ring of graphene. This overlapping known also as a pi-stacking of rings occurs at very small distances between them, having the order of units of nanometers. At such a distance the transition of the electron from the Fermi level of graphene to the LUMO level of the adenine molecule is possible. This transition can happen only in case the energy of the excited light is equal to the mentioned Fermi-LUMO value. It means that such electron transfer is possible only

in case of resonance between these energies. Such electron transfer was reported before for the phthalocyanine molecules deposited on the graphene layer [49].

The estimation of the LUMO level for the adenine molecule is not a trivial task. Usually, it is possible to do it theoretically, but different calculation methods can give varying results. The calculation, by means of the Hartre-Fok approach, gives values, which are definitely too high [48, 49]. Better values of HOMO-LUMO gap for adenine ~ 4eV can be achieved in the case of calculations by using electronic density functional theory [53, 54]. The last numbers were proved in an experiment by authors of ref. [55], who irradiated adenine films by synchrotron radiation and from the results of these experiments determined real and imaginary parts of dielectric permittivities for adenine, which finally allows judging of the energy of the HOMO-LUMO gap to be near 4.4 eV. The exact position of the HOMO and LUMO levels are estimated in the article [55] as -2.2 and -6 eV. Supposing that Fermi level of graphene is near -4.6 eV, it can be constructed as an approximate scheme of the energy levels according to which the electron transfer from graphene to adenine can occur (Fig.26).

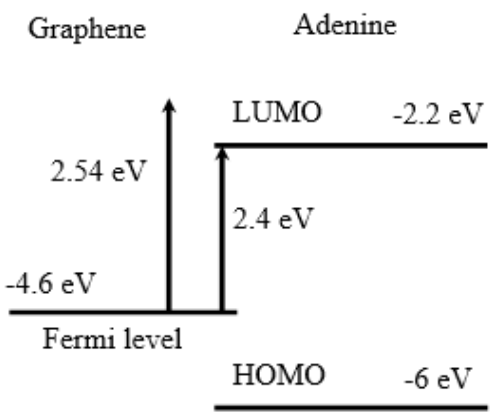

Fig.26 Scheme of electron transfer from graphene to adenine molecule.

According to this scheme, the SERS effect on graphene will be more pronounced for those wavelengths (energies) of excited light, which coincides with the Fermi-LUMO gap. We checked this suggestion by the comparison of the Raman signals of adenine on graphene in the case of 514- and 488 nm excitations. The intensities of the most pronounced Raman bands in the range 1100–1500 cm^{-1} are plotted after the subtraction of the baseline and normalization on the laser intensity for both excitation wavelengths. It can be seen that the light with the photon energy 2.41 eV (514 nm) fits better to the energy gap than the photons with an energy of 2.54 eV (488 nm). As a result, enhancement of the Raman signals for the adenine on graphene is slightly higher in the case of 514 nm excitation wavelength.

One method to control the intensity of the Raman enhancement is correct adjustment of the light excitation to come in resonance with Fermi-LUMO transition. Additionally, there is another way to control the SERS intensity: through the adjustment of the Fermi level of graphene with electrical voltage. This could in principle result in electrically controlled changes in the Fermi-LUMO transition and electrical modulation of the Raman signal from adenine deposited on graphene. The idea itself is quite attractive, but our initial measurements (see Appendix) done for its realization demonstrated several technical complications, which cannot be solved in a strict way:

- The Fermi level of graphene is very sensitive to these molecules, which can be adsorbed on it from the air. Usually, graphene absorbs water vapor from the air. This process occurs very quickly when graphene is stored and operated in room conditions. Practically it means that at room conditions and ambient humidity Fermi level of graphene does not exactly correspond to the -4.6 eV value. To get such value of Fermi level, graphene should be put in a vacuum and heated at the temperature ~ 100^{o}C for several minutes. Then the question of how to combine drop cast deposition of adenine solution with vacuum and high-temperature conditions is presented.
- Exact control of the Fermi level for graphene is possible only when measurements of Volt-Ampere characteristics of graphene field effect transistor are taken, in addition to which, adenine will be deposited. So it implies that vacuum and temperature control should be supplemented by the electrical control of the sample, which in addition allows SERS measurements. This makes experimental setup even more complicated;
- Some authors [56] found the way of realization of electrically controlled Raman on the graphene surface in air conditions. They noted that because of the absorption of the molecules from air, in the Raman intensity vs. voltage dependence there is a huge hysteresis and a certain practice that is needed to catch the desirable SERS effect. The effect is visible only at essentially high voltages 100-150V. In this study, the high voltages applied to graphene caused electrical damage. It seems that the authors of the mentioned paper prepared a lot of samples and published results that included only a few samples, which were not damaged by the high voltage.

Considering the technical difficulties of the various experiments from studies, the difficulties should be overcome in order to construct electrically controlled graphene-based Raman substrate with better performance. This can be one of the objectives of future experimentation.

5. Raman spectra of adenine in SERS

Measurements of Raman signals from small amounts of analyte deposited on the substrate have proven that Raman bands not only from the investigated analyte but also from the underlying substrate can be depicted on the same spectrum. If graphene and silicon play the role of a substrate, it is quite easy to distinguish their characteristic Raman bands from the bands of the analyte. It is because the positions of the Raman bands for silicon and graphene havee been previously identified and are assigned to their certain lattice vibrations. One can see that gold nanoparticles deposited on the surface create quite strong Raman bands, which can hide the useful signal from the adenine (Fig.27).

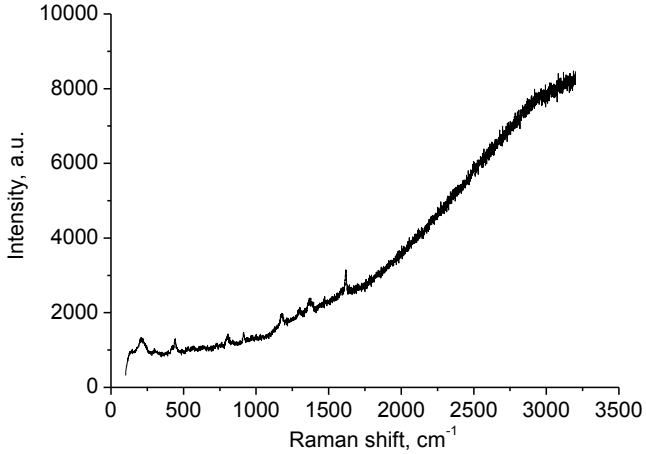

Fig.27 Raman spectrum from a dried droplet of Au-SiO_2 nanoparticles deposited on the glass, excitation wavelength is 633 nm.

Metal itself does not change its polarizability under the influence of the incident light. Therefore, both silver and gold metals do not have characteristic Raman bands. Consequently, the mentioned bands can be caused by the chemicals accompanying the synthesis of gold nanoparticles: ammonia, sodium hydroxide or potassium carbonate. In principal, the re-washing of nanoparticles with high purity water could improve the situation in the sense that extensive washing could reduce the amount of these undesirable compounds and therefore increase the intensity of the Raman signal. However, a part of the nanoparticles inevitably will be lost during this washing procedure. Hence, here we should balance between the number of washings and the desirable concentration of nanoparticles. Since the study of the traces of the mentioned side chemicals is not a goal of the present work, it has been decided to compare the SERS signals of

adenine deposited on silver nanoparticles. Synthesis of silver nanoparticles appeared much clearer, to that of the gold, in a sense that nanosized silver was obtained not chemically but more physically in the high voltage discharge [25]. Besides the fact that the silver nanoparticles also give some bands, which is probably caused by some stabilizing agent (Fig.28), these bands are not overlapped with the spectral range of the adenine bands.

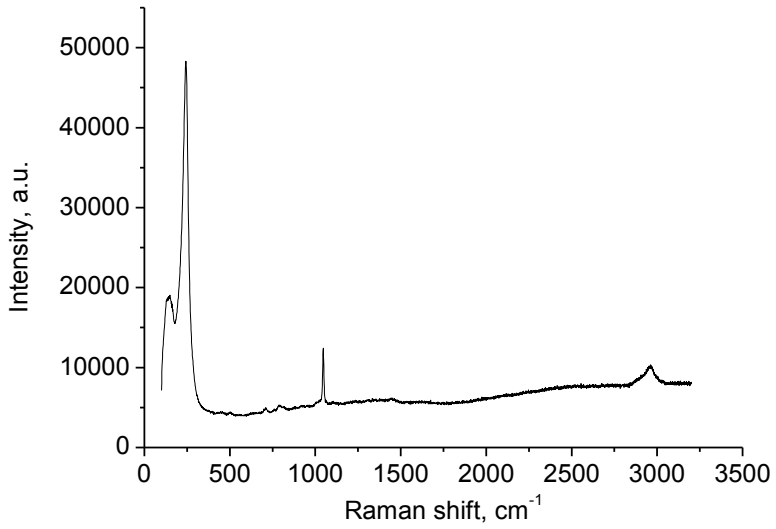

Fig.28 Raman spectrum from dried droplet of silver nanoparticles deposited on the glass, excitation wavelength is 633 nm.

As it was mentioned in the previous section, a water dispersion of silver nanoparticles was dropped on the silicon substrate and formed a kind of circular ring with softly aggregated nano-silver. Then the droplet of adenine solution was dried on the top of this silver ring (Fig.29).

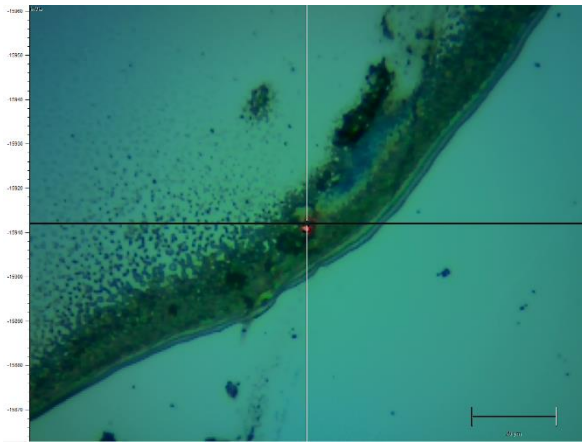

Fig.29 Microscopic image of sequentially drop-casted and dried silver nanoparticles and adenine.

It can be seen that the intensity of the Raman signal from adenine when in contact with the silver ring is almost 2.3 times higher than for the adenine deposited on graphene (Fig.30).

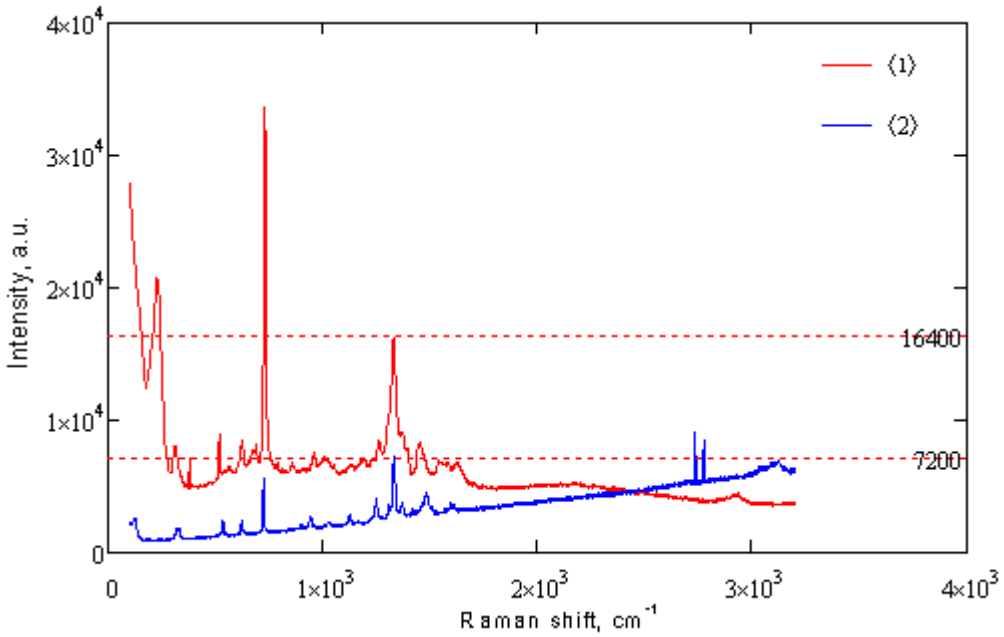

Fig.30 Comparison of the Raman spectra of adenine deposited on silver nanoparticles (1) or graphene (2).

The final comparison of the Raman signals for the adenine deposited on graphene, silver and glass is not an easy task. This is due to the strong background fluorescence. The Raman signal from the adenine on glass or on quartz is hardly recognizable. A red 633 nm laser was used for excitation to decrease parasitic fluorescent background of adenine. Even at 100% (~50mW) of laser intensity the Raman signal from adenine on glass is quite weak on the strong fluorescent background (Fig.31). Indeed, one can check that one of the strongest Raman bands at 1340 cm^{-1}, in this case, has a value near 2000 a.u., if we subtract the background fluorescence. Since the signals for adenine on silver were obtained at 1% of laser intensity, we should divide 2000 a.u. by 100 and obtain 20 a.u. as a result for adenine on glass. Having the adenine on silver at the intensity near 500 a.u. for the same band excited at 1% of laser intensity, it can be concluded that such simple division 500/20 gives enhancement of 25 times.

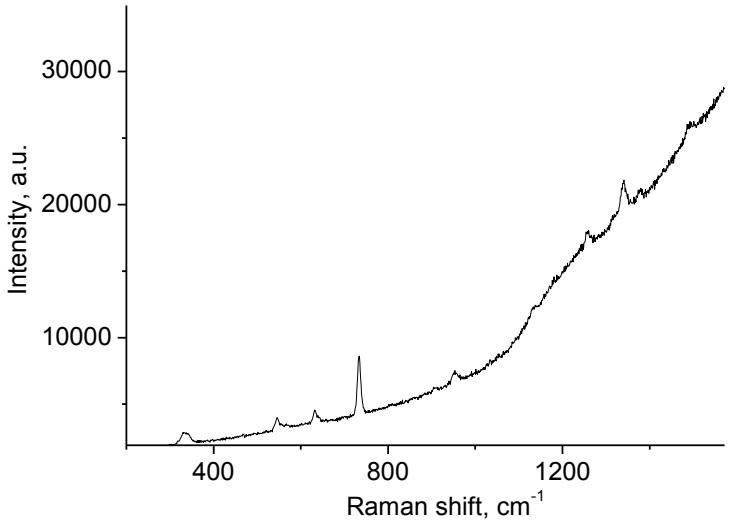

Fig.31 The Raman signal from adenine deposited on a glass substrate.

Literature data frequently referred to several orders of Raman enhancement caused by SERS. Taking this into account, the 25 times obtained in this study is small. An even ratio between the intensity of Raman bands is used in this case. However, some authors reasonably multiply this ratio by the ratio of molecules producing the Raman signal [57]. One can assume that for adenine on glass, the signal is collected from the sample area of several square microns at which laser beam is focused. At the same time, SERS can be given only by adenine molecules sitting in the hot spots between silver nanoparticles and the area of these hot spots can be in the range of several tens of square nanometers. Additional multiplier equal to the ratio of nano and micro areas can give 3 orders more to that 25 times enhancement, which was obtained earlier. In this way, it is possible to recalculate the SERS enhancement to obtain a value, which is closer to the literature data.

Since it is hard to estimate directly the amount of adenine in contact with the hot spots caused by silver nanoparticles, such estimations can be done indirectly after the collection of big amounts of data from the differently diluted adenine solutions. This can be one of the tasks included in future work.

6. Summary

In the course of the present work, several experimental methods for the preparation and optical investigation of samples were mastered. Particularly, microstructures formed after evaporation of differently diluted adenine solutions and dispersions of the noble metal nanoparticles were investigated by means of bright- and dark-field microscopies. Usage of noble metal nanoparticles and graphene as SERS substrates were examined.

Enhanced Raman scattering from thin adenine layers deposited on graphene was detected. It was accompanied by the quenching of the background fluorescence of adenine by the underlying graphene layer. The enhancement of the Raman signal depends on the photon energy of the exciting light in a manner which was in agreement with the assumption that a resonant electron transfer from the Fermi level of graphene to the LUMO level of adenine molecule took place.

Raman enhancement for adenine deposited on the top of noble metal nanoparticles was 2.3 times higher than in the case of graphene. It was because in the case of graphene, there was only chemical enhancement, but when using silver nanoparticles, there was also an electromagnetic enhancement of the Raman signal**.** Direct estimation of the Raman enhancement coefficient was hard because Raman bands were hidden by the background fluorescence and it was not easy to estimate the amount of adenine in the hot spots between the silver nanoparticles. When the Raman bands of adenine were deposited on graphene, an increase of at least 10-12 times was observed. The increase was up to 25 times when deposited on top of silver nanoparticles.

The main results of the present research were published in the Nanoscale Research Letters journal: Dolgov L., Pidhirnyi D., Dovbeshko G., Lebedieva T., Kiisk V., Heinsalu S., Lange S., Jaaniso R., Sildos I., “Graphene-Enhanced Raman Scattering from the Adenine Molecules”, Nanoscale Research Letters, Vol. 11, Issue 197, 2016, doi: 10.1186/s11671-016-1418-5.

7. Kokkuvõte

Käesoleva töö käigus õpiti mitmeid eksperimentaalseid meetodeid proovide valmistamiseks ja optiliseks uurimiseks. Fookuse all olid mikrostruktuuride kujunemine peale aurustumist erinevate adeniinikontsentratsioonidega ja väärismetallnanoosakeste struktuurid, mida uuriti tumevälja ja helevälja mikroskoopia meetodi abil. Väärismetallnanoosakesi ja grafeeni käsitleti SERS substraatidena.

Uuriti ka Raman hajumise signaali tõhusust õhukestelt adeniinikihtidelt grafeeni pinnalt. Sellele kaasnes adeniini taustfluorestsents koos grafeeni alamkihiga. Raman hajumise tõhusus sõltub footoni energiast ergastatud valgusest sellisel viisil, et toimuks resonantne elektroni ülekanne grafeeni Fermi energia tasemelt adeniini LUMO energia tasemele.

Raman signaali tõhusus väärismetallistnanoosakestele sadestatud adeniinilt oli 2.3 korda tõhusam, kui kasutusel oli grafeeni kiht. See on sellepärast, et kui kasutada grafeeni, toimub ainult keemilise mudeli ergastus, kasutades väärismetallistnanoosakesi, on aga lisaks sellele elektomagneetilise mudeli ergastus. Otsest hinnangut Raman ergastuskoefitsendi jaoks on raske anda, kuna Ramani piigid on peidetud taustfluoresentsi poolt ja seega pole kerge määrata adeniini hulka huvipunktides hõbeda nanoosakeste vahel. Kuid vähemalt 10-12 kordne intensiivsuse tõus adeniini Ramani piikidele on mõõdetud grafeenile deponeerimise ja kuni 25-kordne tõus hõbeda nanoosakestele deponeerimise korral.

Põhitulemused antud uuringu kohta on avaldatud Nanoscale Reseach Letters ajakirjas: Dolgov L., Pidhirnyi D., Dovbeshko G., Lebedieva T., Kiisk V., Heinsalu S., Lange S., Jaaniso R., Sildos I., “Graphene-Enhanced Raman Scattering from the Adenine Molecules”, Nanoscale Research Letters, Vol. 11, Issue 197, 2016, doi: 10.1186/s11671-016-1418-5.

8. Appendix

GERS enhancement manipulations

Having graphene as our substrate for adenine is quite useful due to multiple ways of manipulating its enhancement. Subsequently, some of these methods will be discussed.

Change of Fermi level via voltage

As mentioned in chapter 1.5, the chemical model enhancement is dependable on the charge transfer. This charge transfer can be regarded as resonantly matching the Fermi level of metal. Similarly, for GERS enhancement, it is needed to match exciting light energy to the difference of energies between the Fermi level of graphene and the LUMO of the molecule or the HOMO of the molecule and the Fermi level of the graphene. Due to graphene being a semimetal, with zero band gap, it has a possibility to change its Fermi level by inducing a positive or negative voltage (Fig.32). An experiment was conducted with a series of metal phthalocyanine (M-Pc) molecules (M = Mn, Fe, Co, Ni, Cu, Zn) at different molecular energies, used as probe molecules for GERS enhancement with different voltages [58]. From the results, they found that using positive voltage, which increased Fermi level of graphene, produced lower GERS enhancement and negative voltage oppositely. By keeping the system at a constant wavelength they were able to manipulate Fermi level of graphene from -4.98 eV to -4.22 eV. Using bigger voltages would induce electric tunnelling effects.

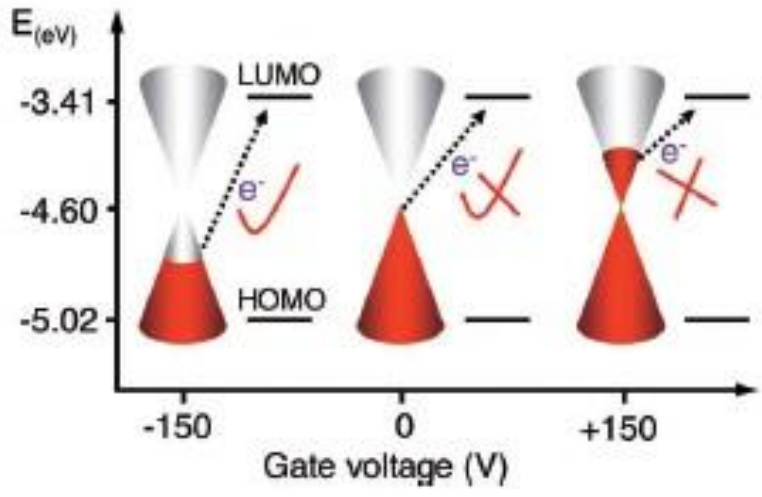

Fig.32 Fermi level modulation of GERS.
The figure is reproduced from ref. [58].

Change of Fermi level manipulation with different impurities

Besides voltage modulation, it is possible to manipulate graphene Fermi level with chemical doping. In the same measurements as above when the system was exposed to atmosphere hysteresis in the voltage shift would occur with different impurities. But by doing a fast sweep with the voltage, this effect would not be so evident. Additional studies in a vacuum and by n/p-doping atmosphere (NH_3 and O_2) had confirmed this [59].

Using different excitation energies

Similarly to Fermi level modulation, it is possible to manipulate the charge transfer mechanism in GERS with the excitation light energies (Fig.8). By using wavelength-scanned Raman excitation spectroscopy, one could find the detailed charge transfer mechanism structure. For example to study GERS wavelength-scanned Raman excitation experiments were implemented (Fig.33). Raman excitation profiles of CuPc molecule were obtained in the range of 545~660 nm and the results implied that GERS enhancement follows ground state charge transfer [60].

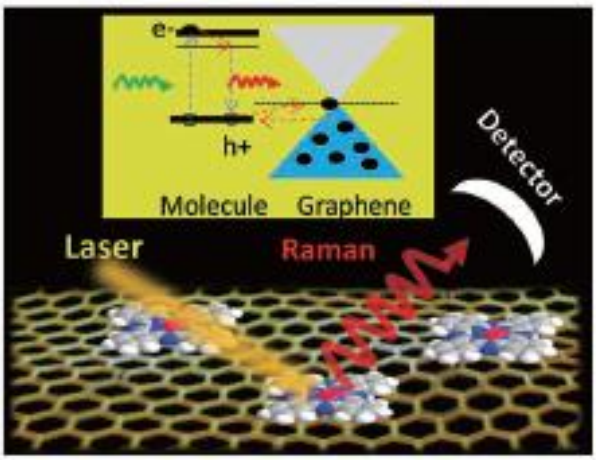

Fig.33 Wavelength-scanned excitation profile of GERS.
The figure is reproduced from ref. [61].

Considering all of the mentioned information and noting that GERS enhancement is similar to SERS chemical model, the main factors for enhancement are:

- To have the molecule really close to graphene, as the chemical enhancement, works only on short-range;
- Molecule orientation with the active sites, for a better charge transfer, should be facing the graphene;
- For resonant charge transfer, the energy difference of the Fermi level of graphene to the HOMO or the LUMO molecule energy level should be equal to the exciting light energy value.

Authors attempt to manipulate GERS enhancement

A setup was devised to study the combination of previously mentioned methods. It consisted of graphene sheets prepared by chemical vapour deposition and transferred on a silicon substrate covered with a 200 nm thick silica layer. The setup had been additionally connected with wires to apply both positive and negative voltages. To use it for Raman spectroscopy, an adenine droplet was placed to partially cover one of the graphene sheets and the silicon substrate (Fig.34). Subsequently, we chose two points: one where adenine covered graphene and the second where adenine covered silica. From each point, the Raman signal measurement was done under three voltage values -45V, 0V and 45V (Fig.35).

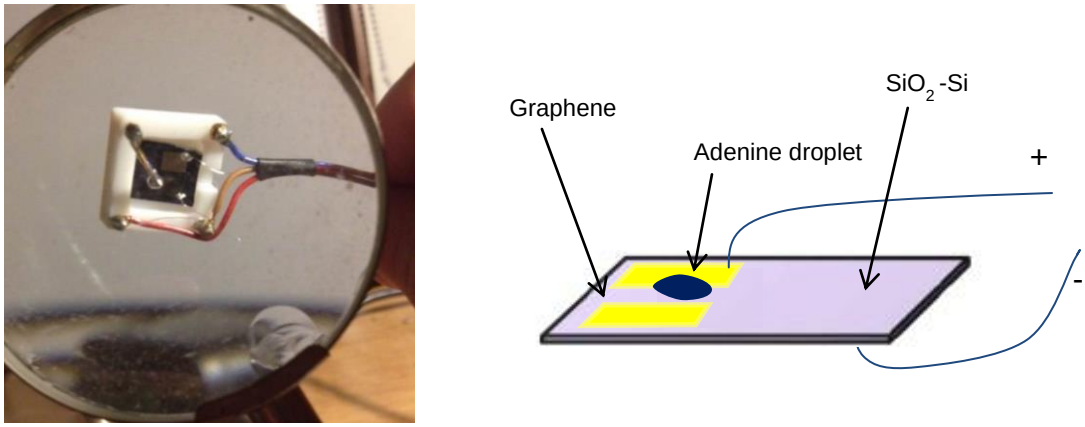

Fig.34 The scheme of the system setup to detect Adenine with a Raman modified technique.

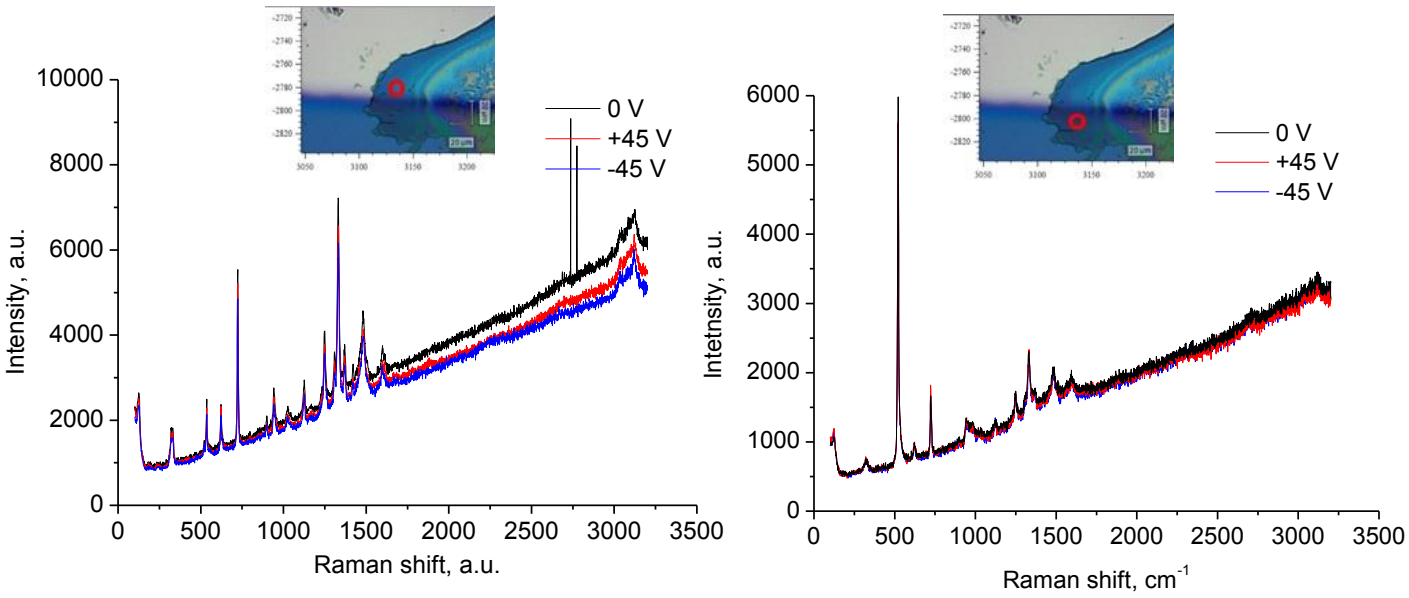

Fig.35 Raman measurements of (a) adenine on the graphene underlying layer and (b) adenine on the SiO_2-Si underlying layer.

One can see two differences by comparing the previous graphs. Firstly, for the adenine signal, which is mainly in the range of 1000-1500 cm^{-1}, the Raman shift is more prominent in the case of adenine on graphene. Secondly, using the voltage shift Raman signal of adenine droplet on SiO_2-Si did not affect it but on graphene, there were slight changes. Comparing the Raman signal of adenine on graphene and on SiO_2-Si we have up to 3 times enhancement.

9. References

[1] Matousek P., Draper E. R., Goodship A. E., Clark I. P., Ronayne K. L., Parker A. W., “Noninvasive Raman spectroscopy of human tissue in vivo.”, Applied Spectroscopy, Vol. 60, Issue 7, pp. 758-763, 2006; doi: 10.1366/000370206777886955

[2] George M. Bodner; James N. Spencer; Lyman H. Rickard, “Chemistry: Structure and Dynamics”, Publisher: Wiley, 2010, ISBN13: 9780470587119

[3] M. Schreiner, M. Strlič, R. Salimbeni, "Handbook on the Use of Laser in Conservation and Conservation Science”, Publisher: COST Office, 2008, ISBN: 9738810930

[4]. Tolles, W. M., Nibler, J. W., McDonald, J. R., Harvey, A. B., "A Review of the Theory and Application of Coherent Anti-Stokes Raman Spectroscopy (CARS)", Applied Spectroscopy, Vol. 31, Issue 4, pp. 253–271, 1977,. doi: 10.1366/000370277774463625

[5] Galyna Dovbeshko, Olena Fesenko, Andrej Dementjev, Renata Karpicz, Vladimir Fedorov, Oleg Yu Posudievsky, “Coherent anti-Stokes Raman scattering enhancement of thymine adsorbed on graphene oxide”, Nanoscale Res Lett., Vol. 9, Issue 1, pp. 263, 2014, doi: 10.1186/1556-276X-9-263

[6] Charles H. Camp, Young Jong Lee, John M. Heddleston, Christopher M. Hartshorn, Angela R. Hight Walker, Jeremy N. Rich, Justin D. Lathia, Marcus T. Cicerone , “High-Speed Coherent Raman Fingerprint Imaging of Biological Tissues”, Nature Photonics, Vol. 8, pp. 627–634, 2014, doi:10.1038/nphoton.2014.145

[7] Jonathan C. White, “Stimulated Raman Scattering”, Topics in Applied Physics, pp. 115-207, 1987, doi: 10.1007/978-3-662-10635-8_4

[8] Renee R. Frontiera, Anne-Isabelle Henry, Natalie L. Gruenke, Richard P. Van Duyne, “Surface-Enhanced Femtosecond Stimulated Raman Spectroscopy”, J. Phys. Chem. Lett., Vol. 2, Issue 10, pp. 1199–1203, 2011, doi: 10.1021/jz200498z

[9] Mansfield, Jessica C. Mansfield, George R. Littlejohn, Mark P. Seymour, Rob J. Lind, Sarah Perfect, Julian Moger, “Label-free chemically specific imaging in planta with stimulated Raman scattering microscopy”, Anal. Chem., Vol. 85, Issue 10, pp. 5055–5063, 2013, doi: 10.1021/ac400266a

[10] George R. Littlejohn, Jessica C. Mansfield, David Parker, Robert Lind, Sarah Perfect, Mark Seymour, Nicholas Smirnoff, John Love, Julian Moger, “In vivo chemical and structural analysis of plant cuticular waxes using stimulated Raman scattering (SRS) microscopy.”, Plant Physiology, Vol. 168, Issue 1, pp. 18–28, 2015, doi: 10.1104/pp.15.00119

[11] Martin R. M., Falicov L. M., “Resonant Raman scattering”, Topics in applied physics, Vol. 8, pp. 79-143, 1983, doi: 10.1007/3-540-11913-2_3.

[12] Smith W., Dent, G. “Introduction, Basic Theory, and Principles and Resonance Raman Scattering” in Modern Raman Spectroscopy – A practical Approach, Publisher: John Wiley & Sons, pp. 93-97, 2005, ISBN: 978-0-471-49794-3

[13] Shinya Yoshikawa , Atsuhiro Shimada, Kyoko Shinzawa-Itoh, "Respiratory Conservation of Energy with Dioxygen: Cytochrome c Oxidase", Metal Ions in Life Sciences, Vol. 15, pp. 89-102, 2015, doi: 10.1007/978-3-319-12415-5_4

[14] E.C. Le Ru, E. Blackie, M. Meyer, P. G. Etchegoin, “Surface Enhanced Raman Scattering Enhancement Factors: A Comprehensive Study”, The Journal of Physical Chemistry C, Vol. 111, Issue 37, 2007, doi**:** 10.1021/jp0687908

[15] Stefan Kruzewski, “Enhancement mechanisms in the SERS phenomenon”, Aspects of Contemporary Optics, Vol. 281, 1998, doi:10.1117/12.301353

[16] Jiang Xudong, Campion Alan, “Chemical effects in surface-enhanced raman scattering: pyridine chemisorbed on silver adatoms on Rh (100)”, Chem. Phys Lett., Vol. 140, pp. 95–100, 1987 , doi: 10.1016/0009-2614(87)80423-2

[17] Semion K. Saikin, Yizhuo Chu‡, Dmitrij Rappoport, Kenneth B. Crozier, and Alán Aspuru-Guzik “Separation of Electromagnetic and Chemical Contributions to Surface-Enhanced Raman

Spectra on Nanoengineered Plasmonic Substrates", J. Phys. Chem. Lett., Vol. 1, Issue 18 18, pp. 2740–2746, 2010, doi: 10.1021/jz1008714

[18] Bhavya Sharma, Renee R. Frontiera, Anne-Isabelle Henry, Emilie Ringe, Richard P. Van Duyne, "SERS: Materials, applications, and the future", Materials Today, Vol. 15, Issues 1–2, pp. 16–25, 2012, doi: 10.1016/S1369-7021(12)70017-2

[19] Roni Lehmann-Werman et al., "Identification of tissue specific cell death using methylation patterns of circulating DNA", PNAS Early Edition, Vol. 113, Issue. 20, 2016, doi: 10.1073/pnas.1519286113.

[20] Novoselov K. S., Geim A. K., Morozov S. V., Jiang D., Zhang Y., Dubonos S. V., Grigorieva I. V., Firsov A. A., "Electric field effect in atomically thin carbon films.", Science, Vol. 306, Issue 5696, pp. 666-669, 2004, doi: 10.1126/science.1102896

[21] Nair R. R.,Blake P., Grigorenko A. N., Novoselov K. S., Booth T. J., Stauber T., Peres N. M. R., Geim A. K., "Fine Structure Constant Defines Visual Transparency of Graphene", Science, Vol. 320, Issue 5881, pp. 1308, 2008, doi: 10.1126/science.1156965

[22] Long Ju, Baisong Geng, Jason Horng, Caglar Girit, Michael Martin, Zhao Hao, Hans A. Bechtel, Xiaogan Liang, Alex Zettl, Y. Ron Shen, Feng Wang, "Graphene plasmonics for tunable terahertz metamaterials", Nature Nanotechnology, Vol. 6, pp. 630–634, 2011, doi:10.1038/nnano.2011.146

[23] Thrall E.S., Crowther A.C., Yu Z., Brus L.E., "R6G on graphene: high Raman detection sensitivity, yet decreased Raman cross-section", Nano Lett., Vol. 12, Issue 3, pp. 1571-1577, doi: 10.1021/nl204446h

[24] Xu W. G., Ling X. L., Xiao J. Q., Dresselhaus M.S., Kong J., Xu H. X., Liu Z. F., Zhang J., "Surface enhanced Raman spectroscopy on a flat graphene surface", Proc. Natl. Acad. Sci. U.S.A., Vol. 109, Issue 24, pp. 9281-9286, 2012, doi: 10.1073/pnas.1205478109

[25] Alexey Treshchalov, Heiki Erikson, Laurits Puust, Sergey Tsarenko, Rando Saar, Alexander Vanetsev, Kaido Tammeveski, Ilmo Sildos, "Stabilizer-free silver nanoparticles as efficient

catalysts for electrochemical reduction of oxygen", Journal of Colloid and Interface Science, Vol. 491, pp. 358-366, 2017, doi: 10.1016/j.jcis.2016.12.053

[26] Stöber W., Fink A., Bohn E., "Controlled growth of monodisperse silica spheres in the micron size range", J. Colloid Interface Sci., Vol. 26, Issue 1, pp. 62-69 , 1968, doi: 10.1016/0021-9797(68)90272-5

[27] Tan Pham , Joseph B. Jackson , Naomi J. Halas , T. Randall Lee, "Preparation and Characterization of Gold Nanoshells Coated with Self-Assembled Monolayers", Langmuir, Vol. 18, Issue 12, pp. 4915–4920, 2002, doi: 10.1021/la015561y

[28] Watson J. D., Crick F. H. C., "Molecular Structure of Nucleic Acids: A Structure for Deoxyribose Nucleic Acid", Nature, Vol. 171, pp. 737–738, 1953, doi: 10.1038/171737a0

[29] Choi S., Park S., Yang S.-A., Jeong Y., Yu J. "Selective self-assembly of adenine-silver nanoparticles forms rings resembling the size of cells", Nature Sci.Reports, Vol. 5, Issue 17805, pp. 1-9, doi: 10.1038/srep17805

[30] Oldenburg S., Westcott S., Averitt R., Halas N., "Surface enhanced Raman scattering in the near infrared using metal nanoshell substrate", J. Chem. Phys., Vol.111, pp. 4729–4735, 1999, doi: 10.1063/1.479235

[31] http://www.rigb.org/our-history/iconic-objects/iconic-objects-list/faraday-gold-colloids

[32] Robert D. Deegan, Olgica Bakajin, Todd F. Dupont, Greb Huber, Sidney R. Nagel, Thomas A. Witten, "Capillary flow as the cause of ring stains from dried liquid drops", Nature, Vol. 389, Issue 23, 1997, doi: 10.1038/39827

[33] Roy P., Huang Y., Chattopadhyaya S., "Detection of melamine on fractals of unmodified gold nanoparticles by surface-enhanced Raman scattering ", J. Biomed. Optics, 19(1) 011002, 2014, doi: 10.1117/1.JBO.19.1.011002

[34] Siiman O., Feilchenfeld H., "Internal Fractal Structure of Aggregates of Silver Particles and Its Consequences on Surface-Enhanced Raman Scattering Intensities", J. Phys. Chem., Vol. 92, pp. 453-464, 1988, doi: 10.1021/j100313a042

[35] Thesis author: Xiaohua Huang, “Gold Nanoparticles Used in Cancer Cell Diagnostics, Selective Photothermal Therapy and Catalysis of NADH Oxidation Reaction”, 2006, URL: https://smartech.gatech.edu/handle/1853/10565

[36] Sambles J. R., Bradbery G. W., Yang F., “Optical excitation of surface plasmons: an introduction”, Contemporary Physics, Vol. 32, Issue. 3, pp. 173-183, 2006, doi: 10.1080/00107519108211048

[37] Antti Matikainen, Tarmo Nuutinen, Tommi Itkonen, Santtu Heinilehto, Jarkko Puustinen, Jussi Hiltunen, Jyrki Lappalainen, Pentti Karioja, Pasi Vahimaa, “Atmospheric oxidation and carbon contamination of silver and its effect on surface-enhanced Raman spectroscopy (SERS)”, Nature Sci. Reports, Vol. 6, Issue 37192, 2016, doi:10.1038/srep37192

[38] Paria S., Chaudhuri R., Jason N., “Self-assembly of colloidal sulfur particles on a glass surface from evaporating sessile drops: influence of different salts”, New J. Chem., Vol. 38, Issue 12, pp. 5943-5951, 2014, doi: 10.1039/C4NJ01267D

[39] Shahidzadeh N, Schut M., Desarnaud J., Prat M., Bonn D. “Salt stains from evaporating droplets”, Nature Sci. Rep., 5:10335 (2015), doi: 10.1038/srep10335

[40] Dongmao Zhang, Yong Xie, Melissa F. Mrozek ,Corasi Ortiz ,V. Jo Davisson , Dor Ben-Amotz, “Raman detection of proteomic analytes“, Anal. Chem., Vol. 75, Issue 21, pp. 5703–5709, 2003, doi: 10.1021/ac0345087

[41] Linards Skuja,” Optically active oxygen-deficiency-related centers in amorphous silicon dioxide”, Journal of Non-Crystalline Solids, Vol. 239, pp. 16-48, 1998, doi: 10.1016/S0022-3093(98)00720-0

[42] Frank L. Galeener, “Band limits and the vibrational spectra of tetrahedral glasses”, Phys. Rev. B, Vol.19, Issue 8, pp. 4292–4297, 1979, doi: 10.1103/PhysRevB.19.4292

[43] Galeener F, Geissberger A., “Vibrational dynamics in ^{30}Si-substituted vitreous SiO_2”, Phys Rev B, Vol. 27, Issue 10, pp. 6199, 1983, doi: 10.1103/PhysRevB.27.6199

[44] Galeener F, Lucovsky G, “Longitudinal optical vibrations in glasses: GeO_2 and SiO_2”, Phys Rev Lett, Vol.37, Issue 22, pp. 1474, 1976, doi: 10.1103/PhysRevLett.37.1474

[45] Russell J., “Raman scattering in silicon”, Appl. Phys. Lett., Vol.6, Issue 11, pp. 223–224, 1965, doi: 10.1063/1.1754144

[46] Parker J., Feldman D., Ashkin M., “Raman scattering by silicon and germanium”, Phys. Rev., Vol. 155 Issue 3, pp. 712–714, 1967, doi: 10.1103/PhysRev.155.712

[47] Ferrari A., Basko D., “Raman spectroscopy as a versatile tool for studying the properties of graphene”, Nat. Nanotech. , Vol. 8, pp. 235–246, 2013, doi:10.1038/nnano.2013.46

[48] Xi L. et al., “Can graphene be used as a substrate for Raman enhancement?”, Nano Lett., Vol. 10, Issue 2, pp. 553–561, 2010, doi: 10.1021/nl903414x

[49] Xu Weigao, Nannan Mao, Jin Zhang., "Graphene: A Platform For Surface-Enhanced Raman Spectroscopy", Small, Vol.9, Issue 8, pp. 1206-1224, 2013, doi: 10.1002/smll.201203097

[50] Mathlouthi M, Seuvre A-M, “F.T.-I.R. and laser-Raman spectra of adenine and adenosine”, Carbohydrate Research, Vol.131, pp. 1–15 (1984), doi: 10.1016/0008-6215(84)85398-7

[51] Randhawa D., Singh M., Kaur I., Bharadwaj L. “Single electron effects in DNA bases”, International Journal of Advanced Engineering Technology, Vol.2, Issue 2, pp. 197-201, 2011, E-ISSN 0976-3945

[52] Randhawa D., Kaur I., Bharadwaj L., Singh M., “Study of HLGS and transfer integrals of DNA bases for investigating charge conduction”, International Journal of Electronics and Communication Engineering & Technology, Vol. 2, No. 1, pp. 43-49, 2011, ISSN 0976-6472

[53] Mishra S. K., Shukla M. K, Mishra P. C., “Electronic spectra of adenine and 2-aminopurine: an ab initio study of energy level diagrams of different tautomers in gas phase and aqueous solution”, Spectrochimica Acta Part A, Vol. 56, pp. 1355-1384, 2000, doi: 10.1016/S1386-1425(99)00262-0

[54] Kilina S., Tretiak S., Yarotski D., Zhu J., Modine N., Taylor A., Balatsky A. "Electronic Properties of DNA Base Molecules Adsorbed on a Metallic Surface", J. Phys. Chem. C, Vol. 111, Issue 39, pp. 14541-14551, 2007, doi: 10.1021/jp070805u

[55] Silaghi S., Friedrich M., Cobet C., Esser N., Braun W., Zahn D., "Dielectric functions of DNA base films from near-infrared to ultra-violet", Phys Stat Sol B, Vol. 242, Issue 15, pp. 3047–3052, 2005, doi: 10.1002/pssb.200562220

[56] Xu H., Xie L., Zhang H., Zhang J., "Effect of graphene Fermi level on the Raman scattering intensity of molecules on graphene", ACS Nano, Vol. 5, Issue 7, pp. 5338–5344, 2011, doi: 10.1021/nn103237x

[57] Hakonen A., Svedendahl M., Ogier R., Yang Z., Lodewijks K., Verre R., Shegai T., Andersson P., Käll M. "Dimer-on-mirror SERS substrates with attogram sensitivity fabricated by colloidal lithography", Nanoscale, Vol. 7, pp. 9405–9410, 2015, doi: 10.1039/C5NR01654A

[58] Xu H. , Chen Y. B. ,Xu W. G. , Zhang H. L., Kong J., Dresselhaus M. S., Zhang J. "Modulating the Charge-Transfer Enhancement in GERS using an Electrical Field under Vacuum and an n/p-Doping Atmosphere", Small, Vol. 7, Issue 20, pp. 2945-2952, 2011, doi: 10.1002/smll.201100546

[59] Ningbo Yi, Chen Zhang, Qinghai Song and Shumin Xiaob, "A hybrid system with highly enhanced graphene SERS for rapid and tag-free tumor cells detection", Scientific Reports 6, Article number: 25134, 2016, doi: 10.1038/srep25134

[60] Caiyu Qiu, Haiqing Zhou, Huaichao Yang, Minjiang Chen, Yanjun Guo and Lianfeng Sun, "Investigation of n-Layer Graphenes as Substrates for Raman Enhancement of Crystal Violet", J. Phys. Chem. C, Vol. 115, Issue 20, pp. 10019–10025, 2011, doi: 10.1021/jp111617c

[61] X. Ling, L. G. Moura, W. G. Xu, M. A. Pimenta, J. Zhang, "Charge transfer in graphene enhanced Raman scattering", J. Phys. Chem. C, Vol 116, Issue 47, pp. 25112–25118, 2012, doi: 10.1021/jp3088447

Lihtlitsents lõputöö reprodutseerimiseks ja lõputöö üldsusele kättesaadavaks tegemiseks

Mina, Siim Heinsalu,

(sünnikuupäev: 21.01.1992)

1. annan Tartu Ülikoolile tasuta loa (lihtlitsentsi) enda loodud teose

“Raman scattering from organic molecules deposited on the noble metal nanoparticles and graphene”,

mille juhendaja on Leonid Dolgov,

1.1.reprodutseerimiseks säilitamise ja üldsusele kättesaadavaks tegemise eesmärgil, sealhulgas digitaalarhiivi DSpace-is lisamise eesmärgil kuni autoriõiguse kehtivuse tähtaja lõppemiseni;

1.2.üldsusele kättesaadavaks tegemiseks Tartu Ülikooli veebikeskkonna kaudu, sealhulgas digitaalarhiivi DSpace´i kaudu kuni autoriõiguse kehtivuse tähtaja lõppemiseni.

2. olen teadlik, et punktis 1 nimetatud õigused jäävad alles ka autorile.

3. kinnitan, et lihtlitsentsi andmisega ei rikuta teiste isikute intellektuaalomandi ega isikuandmete kaitse seadusest tulenevaid õigusi.

Tartus **22.05.2017**